

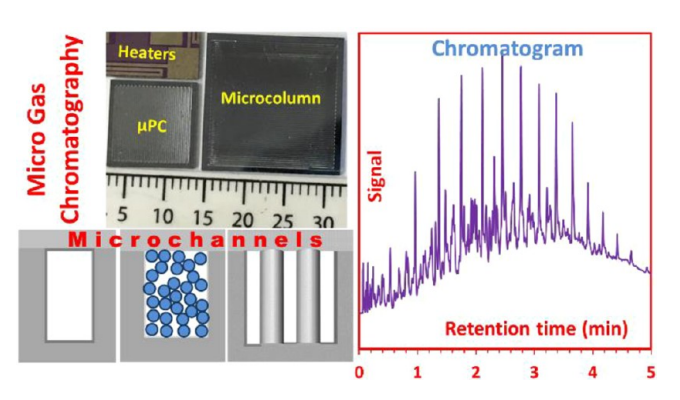
# Micro Gas Chromatography: An Overview of Critical Components and Their Integration

Among a number of gas analyzers, portable gas chromatography (GC) systems created by the integration of microfabricated components are promising candidates for rapid and on-site analysis of a number of complex chemical mixtures. This Feature provides a snapshot of the progress made in developing micro gas chromatography ( $\mu$ GC) systems in the last 4 decades. In particular, we discuss the development of microfabricated preconcentrators, separation columns, and detectors. Furthermore, we review different stationary phase materials used to coat the separation columns and the major efforts toward the development of an integrated  $\mu$ GC.

Bishnu P. Regmi\* and Masoud Agah\*

VT MEMS Lab, Bradley Department of Electrical and Computer Engineering, Virginia Tech, Blacksburg, Virginia 24061, United States

Supporting Information



riven by the rising demands for on-site and rapid chemical analysis of a wide range of complex mixtures, interest in the development of portable or hand-held analytical instruments has significantly increased in the past few decades. On-site chemical analysis provides a number of clear benefits as compared to the laboratory-based measurements. On-site measurements (1) offer rapid analysis and turnaround time for making time-sensitive decisions, (2) assist in the development of effective sampling plans, and (3) minimize the changes in sample composition owing to a number of processes such as evaporation, adsorption, degradation, and oxidation.<sup>1–3</sup>

Among a number of portable devices, a miniaturized version of gas chromatography (GC) system is a very promising technique for rapid and sensitive analysis of complex chemical mixtures. While a conventional GC is a powerful and versatile tool, it is relatively bulky and requires high power with a typical peak power requirement of 2000–3000 V-ampere. Hence, these instruments are normally not field portable. With an aim to develop compact, low power, and field portable GC instruments, considerable research has been conducted over the past 40 years. There has been increased marketability of portable GC instruments, and these products are being developed in both research and commercial laboratories (Table S1 in the Supporting Information). He nomenclature of these

miniaturized GC-based devices is not clear-cut. For example, INFICON 3000 Micro GC (portable model) weighs 36.5 lb, Agilent 490 Micro GC (with 4 channels) weighs 23.4 lb, and Vernier Mini GC Plus (developed by Seacoast Science, Inc.) weighs 2.87 lb, indicating that the use of word "mini" or "micro" is not based on weights. Moreover, the use of the term "micro" is also not based on the type of column used, as miniature GC systems comprising conventional capillary columns are sometimes named as micro GCs.  $^{19,25,26}$  Throughout this article, we use the term "micro gas chromatograph" ( $\mu$ GC) to refer any field portable versions of a GC comprising one or more microfabricated components. A  $\mu$ GC comprises a number of components, including a source of carrier gas, preconcentratorinjector, separation column, detector, pump, valves, and software for instrument control, data acquisition, and analysis.

This feature discusses the theory of (micro) GC, different types of microcolumns and stationary phase materials, preconcentrator, detectors, and a brief history of the development of  $\mu$ GCs. Interested readers are referred to recently published reviews to cover  $\mu$ GC<sup>27–30</sup> or some specific aspects of  $\mu$ GC. <sup>31–34</sup> An extensive and up-to-date review on various microcolumns, stationary phases, and separation performance has been recently published by Ghosh et al. <sup>34</sup>

# ■ THEORY OF (MICRO) GAS CHROMATOGRAPHY

The working principle of  $\mu GC$  is similar to that of conventional GC, except that the different components are miniaturized in  $\mu GC$  to increase portability, decrease power consumption, and increase the speed of analysis. In this section, we briefly discuss chromatographic efficiency, peak symmetry, and peak capacity, which are useful in judging the performance of a  $\mu GC$ . A detailed discussion of basic concepts and terms that are helpful in understanding a gas chromatographic process is given in the Supporting Information.

Published: October 25, 2018



As the components of a mixture move through a separation column, they undergo a number of processes, and hence the components exit the column at different times. Even identical solute molecules, owing to the randomness of different processes, reach the detector at different times leading to a distribution. Additionally, extra column effects, such as injection pulse width and dead volumes, also contribute to the dispersion. Ideally, the separation process results in the generation of a Gaussian-shaped peak. The peak width determines the chromatographic efficiency, which is expressed in terms of the number of theoretical plates or plate number (N). The narrower the peak width is, the greater is the plate number and separation efficiency. The number of theoretical plates is experimentally determined under isothermal conditions using a test solute with a retention factor more than 5.35 Typically, solutes with low values of retention factor exhibit higher plate numbers. Additionally, temperature programming would vastly overestimate the values of plate numbers. The number of theoretical plates increases with the increase in the column length; therefore, chromatographers express the average performance of a column by reporting the number of theoretical plates per meter of column length. Alternatively, the separation efficiency of a column can be expressed in terms of the length of the column that corresponds to one theoretical plate, which is known as height equivalent to a theoretical plate (HETP) or simply plate height (H). The value of H is calculated by dividing the column length (L) by the plate number (N).

$$H = \frac{L}{N} \tag{1}$$

In the 1950s, van Deemter et al.  $^{36}$  made a significant attempt to explain the mechanism of band broadening by using a rate theory and correlated H to a number of different independent sources of sample dispersion. The theory has undergone several modifications since then. In the simplified form, the van Deemter equation can be written as

$$H = A + \frac{B}{\overline{u}} + C\overline{u} \tag{2}$$

where  $\overline{u}$  is the average linear velocity of the mobile phase. In this equation, A accounts for band broadening due to multiple path lengths traveled by the solute molecules through a packed column. This effect is known as "eddy" diffusion; this effect becomes more dominant as the particle size of the packing material increases. The B term considers band broadening due to longitudinal diffusion, and the C term takes into consideration the band broadening due to resistance to mass transfer in the stationary and mobile phases. For an open tubular column, there is no eddy diffusion, and HETP is given by eq 3, which is also known as the Golay equation.

$$H = \frac{B}{\overline{u}} + (C_{\rm S} + C_{\rm M})\overline{u} \tag{3}$$

 $C_{\rm S}$  and  $C_{\rm M}$  represent the mass transfer terms in the stationary and mobile phases, respectively. The complete equation of plate height for an open tubular (i.e., cylindrical) column is given by eq 4.<sup>38</sup>

$$H = \frac{2D_{\rm G}}{\overline{u}} + \frac{2kd_{\rm f}^2\overline{u}}{3(1+k)^2D_{\rm L}} + \frac{(1+6k+11k^2)d_{\rm c}^2\overline{u}}{96(1+k)^2D_{\rm G}}$$
(4)

where  $D_{\rm G}$  is the diffusion coefficient of an analyte in the carrier gas,  $D_{\rm L}$  is the diffusion coefficient of the analyte in the liquid stationary phase, k is the retention factor,  $d_{\rm c}$  is the column diameter, and  $d_{\rm f}$  is the thickness of the liquid film. The theory of open tubular (i.e., circular cross section) are not directly applicable to microfabricated columns with a rectangular cross section. Glenn Spangler<sup>38–40</sup> extended Golay's theory for open tubular GC columns to rectangular columns by redefining average linear velocity and mass transfer term in the gas phase. Spangler was able to obtain more accurate values of  $\overline{u}$  and  $C_{\rm M}$  by better modeling a rectangular column compared to earlier theories. The modified theory correctly predicted experimental HETP data taken from different sources. In simplified form, the Spangler equation is

$$H = \frac{2D_{\rm G}}{\overline{u}} + \frac{2kd_{\rm f}^2\overline{u}}{3((1+k)^2D_{\rm L}} + C_{\rm M}\overline{u}$$
 (5)

 $C_{\rm S}$  is identical for both cylindrical and rectangular columns while  $C_{\rm M}$  is different. For a high aspect ratio (ratio of longer dimension to shorter dimension) columns,  $C_{\rm M}$  is approximately equal to the following expression,

$$C_{\rm M} = \frac{(0.9 + 2k + 35k^2)d^2}{96(1+k)^2 D_{\rm G}}$$
 (6)

where d is the narrower dimension of a rectangular column. It is clear that the resistance to mass transfer term in the gas phase varies with the square of the narrower dimension and independent of the wider dimension. From eqs 5 and 6, it is clear that H can be decreased by decreasing the narrower dimension of a rectangular column. Spangler<sup>38</sup> suggested that the volumetric flow of carrier gas can be adjusted by the wider dimension (or cross-sectional area), and hence by adjusting the volumetric flow, the effects of detector dead volumes could be minimized without compromising the separation efficiency.

Ideally, a chromatographic peak should be symmetrical with a Gaussian shape. However, in reality almost every peak shows some degree of asymmetry, which affects the separation performance. The extent of asymmetry is typically quantified by using two different terms. The pharmaceutical industries use the U.S. Pharmacopeia (USP) tailing factor  $(T_{\rm f})$ , which is defined as

$$T_{\rm f} = \frac{a+b}{2a} \tag{7}$$

where a is the distance from the peak maximum to the front edge of the peak measured at 5% of the peak height, and b is the distance from the peak maximum to the rear edge of the peak measured at 5% of the peak height. Some workers use asymmetry factor  $(A_{\rm s})$  to quantify the peak asymmetry;  $A_{\rm s}$  is defined as

$$A_{\rm s} = \frac{b}{a} \tag{8}$$

where both a and b are measured at 10% of the peak height. When the values are less than 2,  $A_{\rm s}$  and  $T_{\rm f}$  are approximately the same. <sup>41</sup> A tailing factor of 1 indicates a perfectly symmetric peak,  $T_{\rm f}$  less than 1 indicates a fronting peak, and  $T_{\rm f}$  more than 1 indicates a tailing peak. Peak fronting in typically caused by column overloading, while peak tailing is often caused by the strong interactions with the active sites on the surface. Tailing factors between 0.9 and 1.2 are acceptable, and tailing factors up

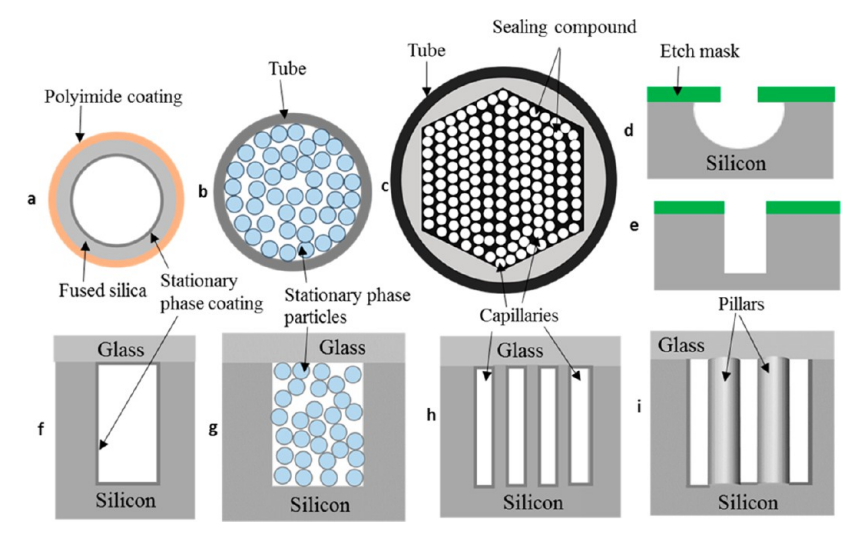


Figure 1. Cross-sectional view of different GC columns and etched profiles: (a) wall-coated capillary column, (b) packed capillary column, (c) multicapillary column, (d) isotropic etch profile, (e) anisotropic etch profile, (f) wall-coated microcolumn, (g) packed microcolumn, (h) multicapillary microcolumn, and (i) pillar-array column.

to 1.5 are often acceptable, but a tailing factor of more than 2.0 indicates some problems that need to be addressed.  $^{41}$ 

Another important parameter that is commonly used to express the separation performance in chromatography is peak capacity  $(n_c)$ , a concept which was originally introduced by Giddings in 1967. 42 Peak capacity of a column is defined as the maximum number of components that can be completely resolved by the column in a defined window of retention time. Giddings used a theory of statistics and demonstrated that the number of components in a random chromatogram cannot contain more than 37% of the peak capacity. 43 In fact, in order to resolve 98% of random components, the peak capacity should exceed the number of components by a factor of 100.44 The separation columns used in  $\mu$ GC are short, and they exhibit low peak capacity for a given analysis. While these columns can separate a sample of moderate complexity, they often fail to resolve the components of a complex mixture. Fortunately, the advent of two-dimensional (2D) chromatography has dramatically increased the peak capacity, thereby enabling the complete separation of complex samples. This technique uses two serially connected columns with orthogonal separation characteristics. The effluents from the first dimension (1D) column are passed to a relatively short second dimension (<sup>2</sup>D) column. Typically, the <sup>1</sup>D column is coated with a nonpolar stationary phase and the <sup>2</sup>D column is coated with a polar stationary phase. When one or several selected portions of the effluent from the first column are subjected to the second dimension separation, the process is called heart-cutting 2D GC. Whenever every portion of the effluent from the <sup>1</sup>D column undergoes a separation in the <sup>2</sup>D column, the process is referred to as comprehensive 2D GC (GC × GC), which was first introduced by Liu and Phillips in 1991. 45 The effluents from the <sup>1</sup>D column are transported to the <sup>2</sup>D column using a transfer system known as a modulator, which traps, focuses, and reinjects the effluents as a pulse at regular intervals. The modulators are broadly divided into two categories: pneumatic and thermal. Pneumatic modulator comprises a sample loop and valve to transfer the sample, while a thermal modulator comprises a segment of capillary column that is cooled for sample collection and is subsequently heated to inject the sample to the other column.<sup>46</sup> The time interval between transfers is known as modulation period or

modulation time. The modulation time is similar or less than the width of the peak emerging from the  $^1\mathrm{D}$  column. The  $^2\mathrm{D}$  column is very short and all the peaks should exit from this column within the modulation time so that there is no remixing of the compounds separated by the  $^1\mathrm{D}$  column. If the two columns are totally orthogonal, the total peak capacity  $(n_{c,2\mathrm{D}})$  (maximum) in GC × GC is given by the product of the peak capacities of the first  $(^1n_c)$  and the second  $(^2n_c)$  dimensions (eq 9). A dramatic increase in peak capacity in the same time frame can be achieved in GC × GC.

$$n_{c,2D} = {}^{1}n_{c} \times {}^{2}n_{c} \tag{9}$$

# SEPARATION COLUMNS

**Types of Columns.** The most critical component of the GC system is the separation column. The cross-sectional view of different types of separation columns used in GC are shown in Figure 1. Conventional capillary columns (Figure 1a—c) are circular in cross section, while chip-based columns (Figure 1f—i), known as microcolumns, are typically rectangular in cross section. Both capillary columns  $^{5,20,21,26}$  and chip-based columns  $^{8-10,47-51}$  have been explored for the use in  $\mu$ GCs. Polyimide-clad fused silica capillary tubing (Figure 1a) is the most widely used capillary column. A major benefit of capillary columns is that, for a given cross-sectional area, they provide higher resolution due to homogeneous coating of stationary phase film along the length of the columns. Alternatively, a number of investigators are working toward the development of microcolumns using different substrates. These devices are typically prepared using microelectromechanical systems (MEMS) technology.

Microcolumns offer a number of clear advantages. The small size of microcolumns enables high speed and low power heating; large-scale batch production of these columns may result in low manufacturing cost; monolithic integration of the columns with other components potentially minimizes the dead volumes and cold spots; and fabrication of regularly arranged support structures inside the channels enhances the separation performance. S1-55 A major limitation, however, of these columns is the accumulation of the stationary phase in sharp corners (known as pooling effect) resulting in nonuniform film thickness inside the

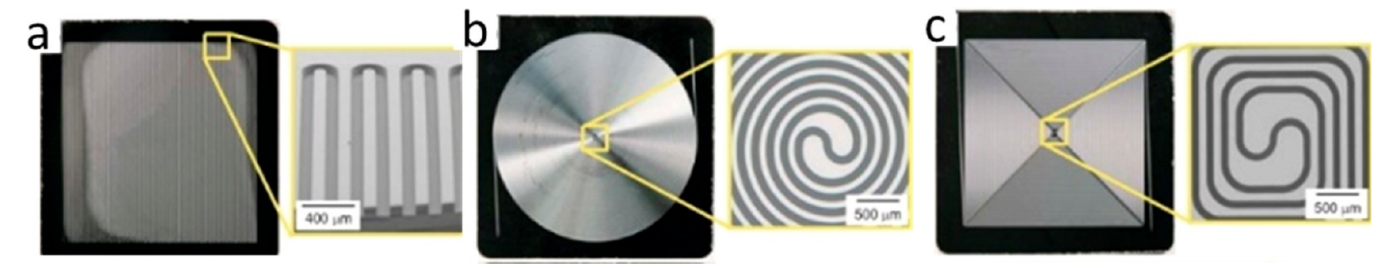


Figure 2. Top-view photographs of three major column layouts: (a) serpentine, (b) circular square, and (c) square spiral. Reproduced with permission from ref 76. Copyright 2010 Elsevier B.V.

column leading to band broadening.<sup>56</sup> Nonetheless, in the case of high-aspect-ratio rectangular columns, the efficiency can be increased by decreasing the width of the channel, and the sample capacity (maximum amount of sample that can injected washout overloading) and flow rate can be increased by increasing the height, thereby offering a possibility of getting better efficiencies compared to conventional capillary columns.<sup>38</sup> Considerable efforts are being made to increase the separation efficiency of the columns by exploring different column architectures <sup>48,51,57–59</sup> and stationary phase coating techniques.<sup>54,60–62</sup>

A longer separation column has to be fit into small footprint (one-meter-long column in a few cm<sup>2</sup> of area) by coiling the microchannels, but this will introduce turns in the channels. A number of different column layouts (also known as column design) are being experimented by the  $\mu GC$  researchers at different institutions. <sup>13,51,53,56,60,63-75</sup> Radadia et al. <sup>76</sup> at the University of Illinois at Urbana-Champaign attempted to compare the separation performance of three popular layouts, serpentine, circular-spiral, and square-spiral designs having all a length of 3 m and a cross section of  $100 \times 100 \,\mu\text{m}$ . The top view of these three designs are displayed in Figure 2. These studies show that gas permeability and unretained solute (methane) band broadening are similar for these three geometries. For a slightly retained iso-octane, the plate numbers were found to be similar for circular-spiral column and square-spiral designs, but an approximately 70% increase in plate numbers was observed for a serpentine design. The authors attribute the enhanced separation performance of the serpentine design to favorable hydrodynamic flow as well as thinner and more homogeneous stationary-phase coating in serpentine configuration. Bhushan et al.,<sup>77</sup> using methane as an unretained marker, showed that circular-spiral and serpentine column layouts exhibit similar flow and band broadening. The band broadening effect for retained compounds was not evaluated.

Silicon wafer is the most widely used material for fabrication of microcolumns. The basic approach for making channels in silicon involves covering the silicon wafer with a mask material (e.g., photoresist), transferring a pattern to the mask material using photolithography and etching the silicon substrate. Two methods, wet etching and dry etching, have been used to create microchannels in silicon substrate. In wet etching process, a liquid solution is used to dissolve the material to form the channels, while in dry etching process, reactive ions or vapor etchant is used. The etching process can be isotropic where the etching rate is the same in all spatial directions or anisotropic where the etching rate is different in directions. The schematic etch profiles produced by isotropic and anisotropic etching are shown in Figure 1d,e. The most common etchant for wet isotropic etching is a mixture of hydrofluoric acid, nitric acid, and acetic acid, while potassium hydroxide or tetramethylammonium hydroxide are the common anisotropic wet etchants for silicon. The dry etching technique, which is commonly used for column fabrication, is deep reactive ion etching (DRIE). After etching, the channels are hermetically sealed using a glass wafer. Strong bonds between silicon and glass are created under the influence of high temperature and an external electric field. In this process, which is known as anodic bonding, the bonding parts are heated at a temperature between 300 and 600 °C, and the silicon is connected to positive terminal and glass is connected to the negative terminal of a high voltage dc (200-2000 V). <sup>78</sup> Resistive heating elements and temperature sensors can be incorporated on the separation columns for rapid temperature ramping under low power conditions. 79,80 Siliconglass microcolumns contain active sites that cause unwanted adsorption of analytes, particularly polar compounds, leading to peak tailing. Typically, these columns are deactivated by treating the columns with different reagents either before or after stationary phase coating to increase the peak symmetry. 81-83 While majority of reported studies have used silicon microcolumns, numerous attempts have been made to explore alternate materials for microcolumns.

Several investigators have utilized metals, such as nickel.  $^{64,84,85}$  steel,  $^{86,87}$  and titanium,  $^{88}$  as a substrate to fabricate microcolumns. Researchers at Louisiana State University in joint efforts with the researchers at the Sandia National Laboratories (SNL) have developed high-aspect-ratio columns with electroplated nickel using LIGA (X-ray lithography, electroplating, and molding) fabrication technique. 64,85 However, the separation performance of these columns have not been fully evaluated. Lewis and Wheeler<sup>84</sup> at SNL developed a nonplanar column using a planar nickel substrate containing circular through holes using a LIGA process. Multiple planar substrates were stacked with their through holes aligned to form longer single-capillary or multicapillary columns. These columns were used for the separation of polar as well as nonpolar analytes. Adkins and Lewis<sup>89</sup> from Defiant Technologies, Inc. recently proposed a "folded passage column" which is formed by an assembly of perforated plates made of a metal, ceramic, or plastic. FROG-4000 portable GC from Defiant Technologies comprises a microcolumn made up of an assembly of etched steel plates, but the details have not been disclosed.<sup>87</sup> One of the most common ways of deactivating the metal surfaces is by depositing a thin film of silicon.85,86

A few studies have attempted to fabricate microcolumns using polymeric materials. Researchers at Georgia Tech fabricated microcolumns using parylene (poly(*p*-xylylene)).<sup>65</sup> These columns were prepared by first depositing parylene both in silicon microchannel mold and on a flat glass surface. Afterward, these parylene-coated devices were glued by parylene-parylene bonding using heat and pressure. Following the bonding, the

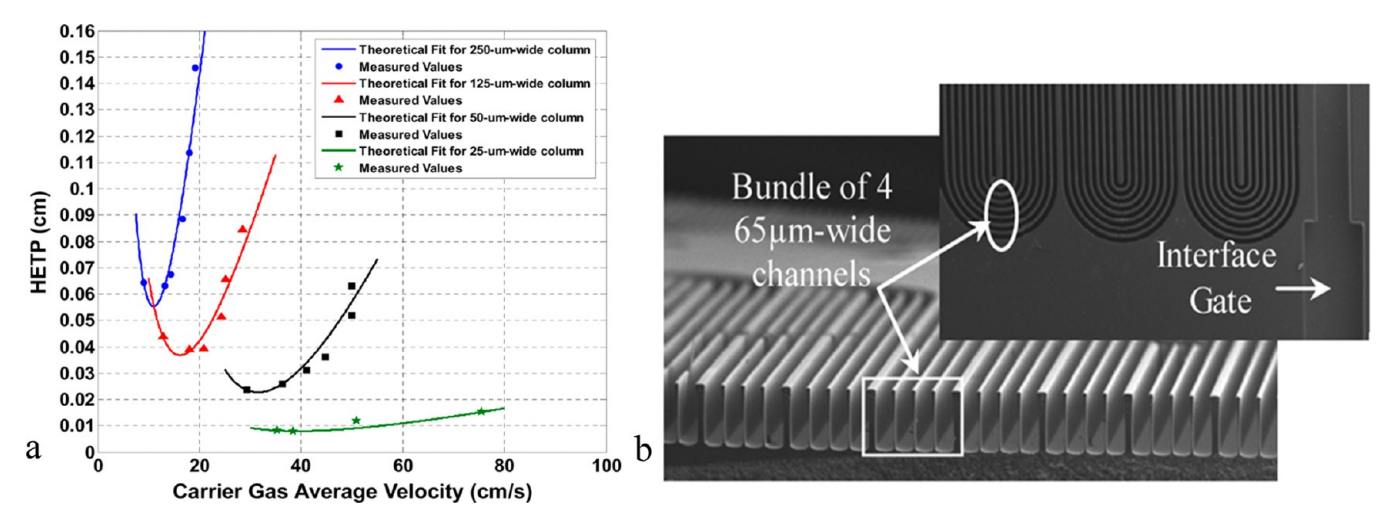


Figure 3. (a) Golay plots for high-aspect-ratio columns of different widths and (b) an SEM image of cross-sectional view of a four-channel MCC; inset is showing the top view. Reproduced with permission from ref 96. Copyright 2009 IEEE.

glass and silicon mold were removed to get freestanding parylene columns. These columns were coated with different polymers as a stationary phase. The parylene columns exhibited faster heating/cooling rates and lower power consumptions compared to silicon-glass columns. However, the separation efficiency, i.e., experimental plate numbers of these columns were very low ranging from 2.2 to 4.8% of the theoretical values, thereby limiting the applications of the parylene columns. Malainou et al. 66 fabricated a polydimethylsiloxane (PDMS) column through molding technique and used the column to separate a mixture of benzene and xylene. While PDMS could be used as a structural material as well as the stationary phase, the column was found to suffer from severe band broadening. Along the same line, Rankin and Suslick<sup>67</sup> developed a disposable microcolumn using a thermoset polymer composite. The microcolumn was fabricated using a reusable mold that was prepared by micromachining of a polymer. While the authors were able to decrease the band broadening, the separation efficiency is not on par with those of silicon columns.

Lewis et al.<sup>91</sup> developed a glass—glass microcolumn with a circular cross section. Two matching glass plates were first etched using hydrofluoric acid to give hemispherical channels, and these glass plates were cold bonded with channels aligned to form spherical channels. The glass plates were strongly held through van der Waals forces. These columns were utilized for the separation of nonpolar compounds. Recently, there has been motivation toward the development of silicon—silicon (all silicon) microcolumns.<sup>92,93</sup> The bonding has been accomplished by a gold diffusion eutectic bond which requires an intermediate layer of gold. The replacement of Pyrex glass with silicon has potential to minimize peak tailing, provide more uniform temperature profile and reduce the power consumption. <sup>92,93</sup> There have been some interest in the use of ceramics as a substrate for microcolumns. <sup>94,95</sup>

The major considerations in the design of microcolumns are analysis time, separation efficiency, pressure drop, and sample capacity. Column dimensions, column-operating temperature, flow rate, and the type of carrier gas influence the separation performance. Optimization of one factor cannot be achieved without compromising other factors. For example, choosing a longer column will increase the resolution but at the same time increases the analysis time. On the other hand, decreasing the film thickness increases the speed of analysis but with a decrease

in sample capacity. The choice of these parameters is dependent on the nature of the mixture to be separated. High-aspect-ratio rectangular columns are very commonly used, because the sample capacity and flow rate can be increased by increasing the height (longer dimension), while the separation efficiency is controlled by the width (shorter dimension). <sup>38,69,85</sup>

The chromatographic performance is dependent primarily on the separation efficiency, which can be enhanced by decreasing the width of a column. For example, Figure 3a shows theoretical and experimental values of HETP as a function of carrier gas velocity, i.e., Golay plots, for four columns of different widths. It is evident that the column efficiency increases, optimum velocity increases, and the Golay plot becomes flatter as the column width decreases. However, a decrease in column width leads to a decrease in sample capacity. A way to evade the limitation of sample capacity is to use a multicapillary column (MCC), which comprises a bundle of several capillaries (Figure 1c) with (nearly) identical retention characteristics coupled in parallel, an idea originally suggested by Golay in 1975. 97 MCCs are commercially sold by Multichrom, LLC (http://www.mccchrom.com). Our group extended the concept of MCC to silicon chips and fabricated two-, four-, and eight-channel MCCs. 96 Figure 3b shows SEM images of cross-sectional side view and top view of a four-channel multicapillary column developed in our lab. 96 One of the major drawbacks of a MCC is polydispersity effect; even a small change in channel-to-channel length, width, and stationary film thickness dramatically effects the band broadening.9

Our group has shown some success in overcoming the challenges associated with MCCs by developing microfabricated pillar-array columns, named as "semipacked columns" (SPCs). <sup>59,63</sup>The SPCs comprise an array of microfabricated posts (square or circular cross section) inside the channels of the columns. In fact, the concept of pillar-array columns was originally proposed by the Regnier group at Purdue University 2 decades ago, <sup>55</sup> and the Desmet group further developed these columns for liquid chromatography. <sup>95,100</sup> The use of pillar-array columns is relatively new in GC. The SEM images of a portion of semipacked column developed by our group are displayed in Figure 4a,b. The presence of micropillars increases the surface area, thereby increasing the sample capacity. Additionally, the micropillars decrease the mass transfer distance resulting in higher separation efficiencies. Several other research groups

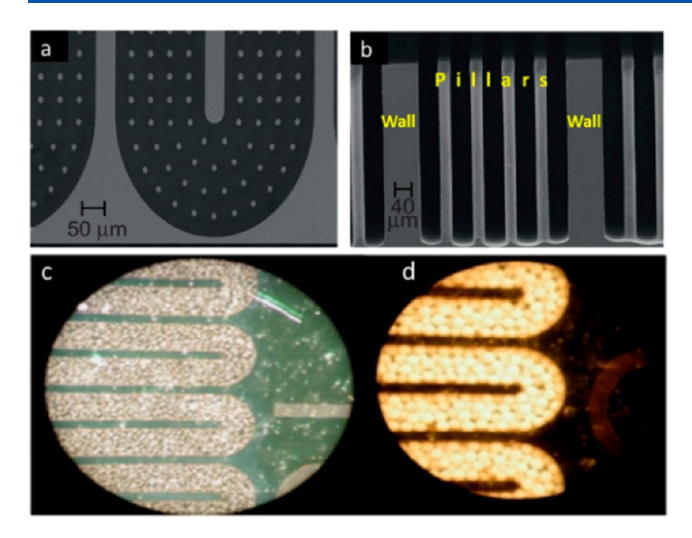


**Figure 4.** Semipacked and packed microcolumns: (a) an SEM image of top view of the channel 20  $\mu$ m circular posts of a portion of an SPC, (b) an SEM image displaying high-aspect-ratio pillars, (c) packed column with Carbopack particles, and (d) packed column packed with HayeSep A beads. The column layout is serpentine in both the cases. Reproduced from ref 107 for parts a and b, and with permission from ref 53 for parts c and d. Copyright 2015 Springer Nature (for parts a and b) and Copyright 2010 IOP Science (for parts c and d).

have also adopted semipacked columns for different studies. 50,57,58,101-103 Very recently, the Desmet group designed efficient separation columns by using radially elongated pillars (REPs) as shown in Figure 5. 48 REPs are elongated perpendicular to the direction of flow and they provide a longer path for the gas to travel mimicking the increased length of columns, thereby achieving a high number of plates. While majority of the reported studies have used wall-coated (or wall-and pillar-coated) open-tubular microcolumns, relatively few studies have described the packing of stationary phase particles inside the channels of microcolumns (Figure 4c,d). 53,73,104,105 Packed columns offer high sample capacity; however, they

require high inlet pressure and provide low speed of separation.  $^{106}$ 

**Stationary Phases.** There has been ongoing interest in the design and evaluation of new stationary phases for microcolumns. Historically, wide range of materials have been explored as stationary phases in microcolumns. For packed columns, polyethylene glycol (PEG)-coated graphitized carbon black (e.g., carbograph), <sup>15,73</sup> graphitized carbon black (e.g., carbopack), <sup>53</sup> porous polymer beads, <sup>53,105</sup> and carbon molecular sieves (e.g., carboxen 1000) <sup>104</sup> have been employed, particularly for the separation of permanent gases and light hydrocarbons.

Much wider variety of materials have been tried as stationary phases in open and semipacked columns. PDMS and its derivatives (under different trade names, e.g., OV-1, OV-101, OV-5, OV-215, and SE-54) have been predominantly used to coat microcolumns by different researchers. 9,47,49,56,63,70,72,74,82,83,85,108-111 Among other polymers, PEGs (trade name Carbowax) have been frequently used because of their ability to separate polar compounds 111-113 Microcolumns are coated using static 49,56,63,83,85,108 as well as dynamic methods. 72,82,103,110 In static coating method, the entire column is filled with a dilute solution of a stationary phase in a volatile solvent by means of a pressurized gas. One of the ends of the column is then sealed, and the solvent is evaporated under vacuum through the other end. Static coating produces a more uniform coating, and the coating thickness can be easily calculated by employing the surface area of the column, concentration of the stationary phase in the solution, and the density of the coating solution.  $^{108}$  However, the major concern is the formation of bubbles during solvent evaporation requiring extreme precautions during the coating process. 49,74,103,114 Recently, Ghosh et al. 49 statically coated a 5.9 m long microcolumn by pressurizing the filled column to 100 psi for 1 h before vacuum-evaporation of the solvent. Our own preliminary experiments have supported this observation. Pressurizing the solution causes trapped air bubbles to dissolve, thereby preventing the formation of air bubbles during vacuum evaporation. An alternate coating method that has been often

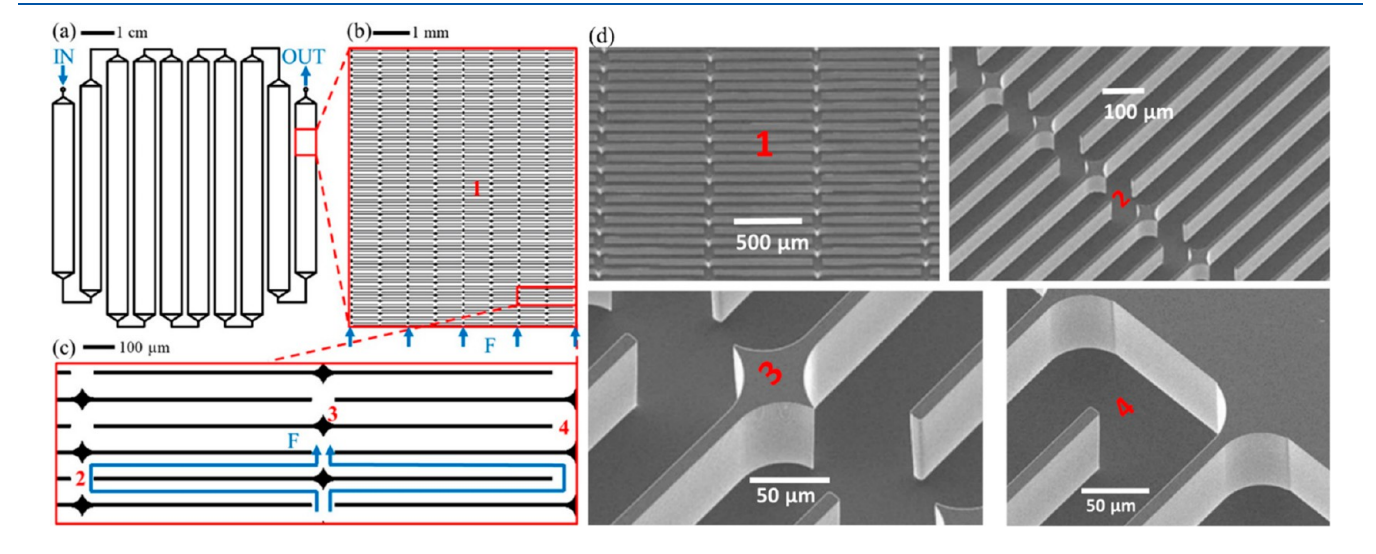


**Figure 5.** Chip-based REP array column developed by the Desmet group: (a) global overview, (b) magnified view of the selected region of part a showing the arrangement of pillars inside the channels, (c) magnified view of the selected region of part b with blue arrows F showing the flow paths, and (d) SEM images of the column structure where the numbers correspond to the locations 1–4 indicated in parts b and c. Reproduced and modified with permission from ref 48. Copyright 2017 American Chemical Society.

used is the dynamic method where a plug of a solution of stationary phase is introduced into the column, and the plug is forced through the column using an inert gas and the rest of the solvent is evaporated by continued gas flow. The film thickness can be altered by changing the concentration of solution and the plug velocity. The dynamic coating method is fast, but the advanced prediction of the film thickness is difficult. One limitation of both of these methods for coating microcolumns is the accumulation of the stationary phase at the sharp corners (known as the pooling effect) resulting in the band broadening. Some success in minimizing the pooling effect has been achieved by rounding the walls using isotropic etching after the DRIE process.<sup>51</sup> Microcolumns often exhibit tailed peaks. Nishino et al.83 statically coated a deactivated silicon-glass microcolumn and capillary column with 5% phenyl-95% methylpolysiloxane stationary phase. The authors observed no peak tailing for the capillary column, but the chip-based column showed tailing for polar compounds (i.e., alcohols and amines) and no tailing for nonpolar compounds (i.e., n-alkanes). Some reports suggest that peak tailing can occur even for n-alkanes.<sup>101</sup> Peak tailing in microcolumns is primarily due to surface adsorption. 81-83,115

Over the years, there have been parallel studies in the development of more homogeneous stationary phase films by employing solid-phase materials and alternate coating techniques. One of the earliest studies was conducted by Kolesar and Reston in the 1990s. 60,116 This work involved the deposition of a 200 nm thick nearly homogeneous film on the walls of a microcolumn by subliming copper phthalocyanine under vacuum prior to anodic bonding of silicon and Pyrex glass. These columns have been used for separation of a binary mixture composed of ammonia and nitrogen dioxide. Carbon nanotubes, because of higher surface-to-volume ratio and thermal stability, have been investigated as a stationary phase in microcolumns. Carbon nanotubes have been grown at the bottom of the separation channel by chemical vapor deposition prior to bonding the silicon chip with glass, and these columns are shown to be useful for ultrafast separation of light alkanes and other simple mixtures. 75,117 Another solid-phase material that has been collectively and reproducibly deposited using the sputtering technique is silica, and these films have been used in rapid separation of light aliphatic hydrocarbons. 54,58 Figure 6 depicts a chromatogram for the separation of a mixture 9 n-

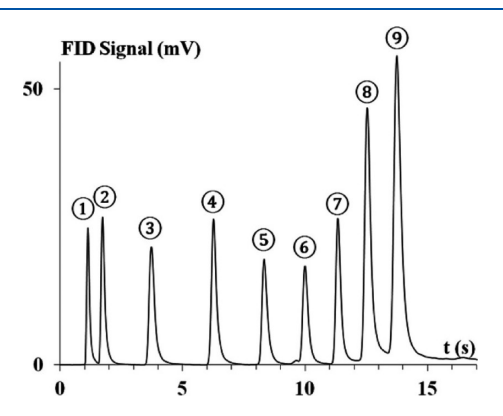


**Figure 6.** Separation of nine linear alkanes using a silica-sputtered column (2.2 m  $\times$  100  $\mu$ m  $\times$  100  $\mu$ m; thickness of silica 3  $\mu$ m). Peak numbers correspond to (1) methane, (2) ethane, (3) propane, (4) butane, (5) pentane, (6) hexane, (7) heptane, (8) octane, and (9) nonane. Reproduced with permission from ref 54. Copyright 2013 American Chemical Society.

alkanes in less than 15 s using a 2.2 m long silica-sputtered microcolumn developed by Haudebourg et al.<sup>54</sup> In addition to silica, these researchers have also investigated sputtered graphite and alumina as a stationary phase for the separation of light alkanes. 54,118 Our group has been successful in the development of thin films of alumina by atomic layer deposition. 61,119,120 The alumina films have been prepared by the reaction of trimethylaluminum and water on the surface of silicon at high temperature (250-300 °C) prior to anodic bonding. The surface -OH groups of alumina can be deactivated by treating the column with a dilute solution of chloro(dimethyl)octadecylsilane after anodic bonding. These films have been found to be promising for the separation of aliphatic and aromatic hydrocarbons. Despite a more homogeneous film formation, the separation efficiency and peak symmetry, of these solid-phase materials in general do not exceed the performance of the columns coated using conventional static or dynamic methods. 58,61,81,115

Recently, there has been interest in the development of monolayer-protected gold, i.e., a gold coated with a onemolecule-thick film of a compound as stationary phase in GC. The original work in this field was conducted by Gross and coworkers. The authors coated commercial circular cross section and square cross section (a model for microcolumn) silica capillary with octadecanethiol-protected gold nanoparticles (GNPs) for high-speed and efficient separation of different class of compounds. While octadecanethiol-protected GNPs are nonpolar, more polar stationary phases were also produced using 4-chlorobenzenethiol-protected GNPs and 4-(trifluoromethyl)benzenethiol-protected GNPs. 122 Inspired by this work, our group has developed monolayer-protected gold as a stationary phase in microcolumns. <sup>62,123</sup> A thin layer of gold have been deposited on the surface of the channels through electroplating, 123 physical vapor deposition, 62 or layer-by-layer deposition of gold nanoparticles<sup>62</sup> prior to anodic bonding. Following the anodic bonding, the surface of gold has been functionalized using a dilute solution of octadecanethiol, which forms a self-assembled monolayer through sulfur-gold interactions. These columns have been shown to be attractive for the separation of saturated hydrocarbons. The separation efficiency of these columns is, however, not as high as that observed with a dynamically coated microcolumn. 62,

Two promising classes of materials that have recently attracted much attention as stationary phases in microfabricated columns are metal-organic frameworks (MOFs)<sup>124</sup> and room temperature ionic liquids (RTILs). 47,103,115 MOFs are porous crystalline materials formed by coordination of metal cations and multidentate organic ligands. MOFs possess high thermal stability, tunable adsorption affinities, high surface area, and uniformly structured cavities. 125 They have already been used in conventional capillaries as attractive stationary phases for highresolution separation of, among others, xylene isomers, polyaromatic hydrocarbons, polychlorinated biphenyls, and various racemates. 125-127 Realizing the importance of MOFs, investigators from SNL have recently utilized HKUST-1, a copper-based MOF, to separate light hydrocarbons present in natural gas, which are otherwise challenging to separate using conventional stationary-phase materials. 124 The MOF film has been prepared by layer-by-layer deposition. Figure 7 shows a high-resolution separation of challenging compounds-methane from ethane and butane from isobutane—present in natural gas using HKUST-1 film. 124 RTILs are liquid organic salts, which have already garnered widespread attention in separation

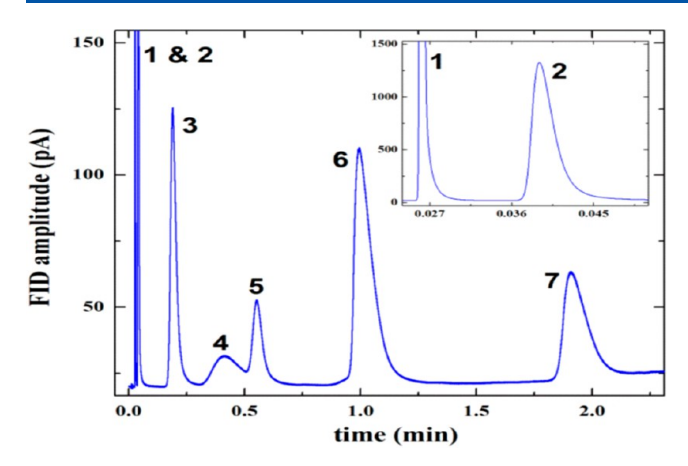


**Figure 7.** Chromatogram showing the complete separation of natural gas using HKUST-1 coated 120 cm x 685  $\mu$ m  $\times$  70  $\mu$ m  $\mu$ GC column. Peaks correspond to (1) methane, (2) ethane, (3) propane, (4) isobutane, (5) n-butane, (6) n-pentane, and (7) n-hexane. Neat n-pentane and n-hexane were added to a natural gas mixture before separation. Figure courtesy of Sandia National Laboratories.

and other analytical applications. RTILs show a multitude of solvation interactions and these interactions can be easily tuned, and hence these materials can be easily tailored to the separation of desired mixtures. Apart from 1D GC, these compounds show attractive features for multidimensional GC. <sup>128,129</sup> RTILs are polar and possess high viscosity, high thermal stability, and low vapor pressure making them attractive stationary phases in the GC. RTIL-coated capillary columns have been commercialized, and they have been extensively employed in the separation of a wide variety of complex chemical mixtures, including but not limited to essential oils, petroleum products, fatty acid methyl esters, and various enantiomers. <sup>129–133</sup> The application of RTILs as stationary GC phases has been reviewed in depth in recent publications <sup>35,134</sup> and a book chapter. <sup>135</sup> While RTILs are established stationary phases for capillary columns, they have not been used in microcolumns until very recently. The Zellers

group deposited a tricationic RTIL in a microcolumn and employed it as a  $^2\mathrm{D}$  column in a comprehensive 2D micro GC ( $\mu\mathrm{GC}\times\mu\mathrm{GC}$ ). Our group recently deposited two commercial RTILs inside semipacked columns for the separation of mixtures comprising both polar and nonpolar compounds.  $^{103,115}$  We observed good separation efficiency, which was found to increase on pretreating the silicon surface with alumina prior to the deposition of an RTIL. Figure 8 shows the chromatograms for the separation of a 21-component mixture using columns coated with 1-butylpyridinium bis-(trifluoromethylsulfonyl)imide on alumina and silicon surfaces. The chromatographic peaks were found to be symmetrical for the tested compounds.

Column Heating Technologies. In a GC column, there exists an equilibrium of analytes between the mobile and stationary phases which is influenced by the column temperature. If a separation is carried out under isothermal conditions at low temperatures, the weakly retained solutes will be reasonably separated while strongly retained compounds show severe band broadening and long retention times. Conversely, a separation conducted under higher isothermal temperatures causes a good separation of strongly retained compounds but a poor separation of weakly retained species. This general elution problem can be solved by temperature programming of the column. In conventional GCs, the column is typically heated by placing it in a bulky air-bath oven which consumes high power and provides only moderate temperature ramp rates. Conventional ovens are routinely used to evaluate the performance of microcolumns; 48,82,103,136 however, they are not suitable for inclusion in portable GC systems. An alternate heating technology that has been widely practiced is resistive heating which has been reviewed in depth by Wang et al.31

Resistive heating involves passing an electric current through a conductor known as heating element. One approach is to use the column as the heating element. In this case, the column is either made of a metal, such as stainless steel, <sup>137</sup> or the surface of the column is coated with a conducting material, such as

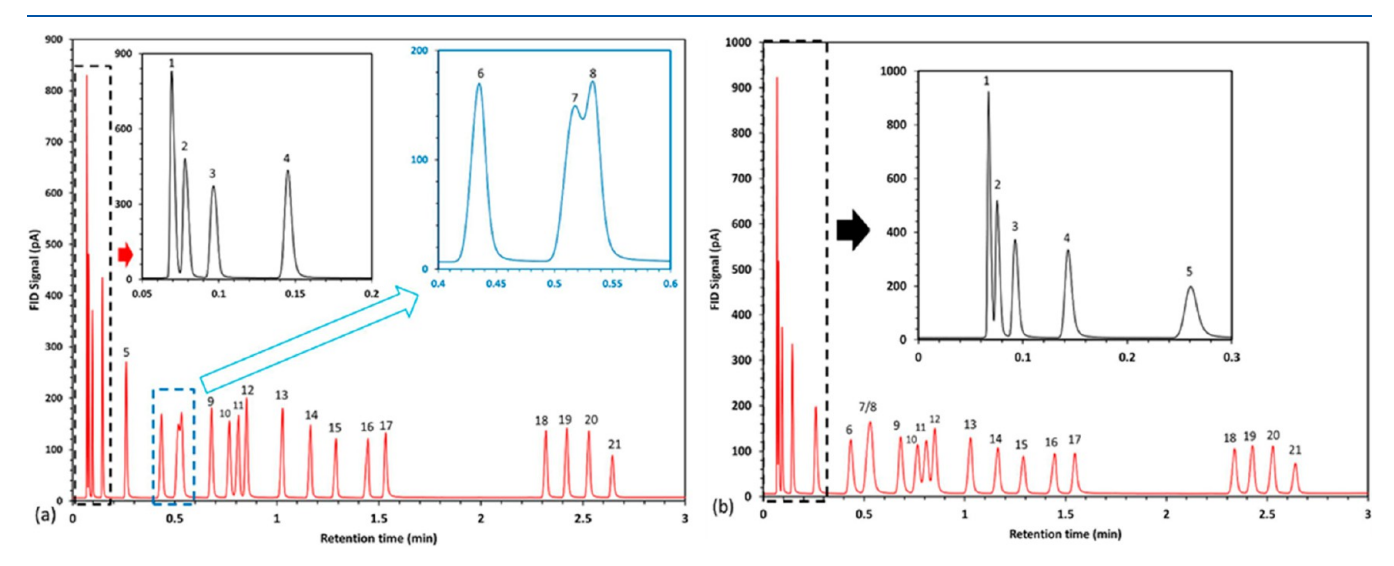


Figure 8. Chromatograms showing the separation of a 21-component mixture using semipacked columns coated with 1-butylpyridinum bis(trifluoromethylsulfonyl)imide on (a) alumina surface and (b) silicon surface. Insets show magnified view of the selected regions. Peak assignments: (1) heptane, (2) octane, (3) nonane, (4) benzene, (5) toluene, (6) ethylbenzene, (7) p-xylene, (8) m-xylene, (9) o-xylene, (10) 2-chlorotolune, (11) isobutylbenzene, (12) styrene, (13) butylbenzene (14) 1,2-dichlorobenzene, (15) 2,5-dichlorotoluene, (16) 1,2,4-trichlorobenzene, (17) benzyl chloride, (18) naphthalene, (19) 2-nitrotoluene, (20) 3-nitrotoluene, and (21) 4-nitrotoluene. Reproduced with permission from ref 115. Copyright 2018 Elsevier B. V.

aluminum. 138 A commercial system that uses direct resistive heating of metal column is the zNose system of Electronic Sensor Technology. 139 Other resistive heating designs that have been commercialized are coaxial and collinear heating designs. In the coaxial design, the column and a sensor wire are passed through a tubular heating element and the whole assembly is insulated; in the collinear design, a heating wire, sensor wire, and column are inserted together into an insulating tube. 140 The collinear design has been used by Fan and co-workers at the University of Michigan (UM) in their portable GC systems. 11,12 Researchers at SNL developed and patented resistive heating technology for microfabricated columns.<sup>79</sup> A thin layer of resistive heating element such as a refractory metal or lightly doped semiconductor is deposited on at least one surface of the substrate (silicon or any other column material). A temperature sensor, which is made of a thermistor material, is also deposited on the column surface. Additionally, the system comprises a control board for electrical control. The column is thermally insulated from its surroundings, thereby improving thermal time response and power consumption. This type of resistive heating system has been adopted by other researchers. 9,75,80,92,141,14 Another heating approach developed and patented by SNL involves heating the column by keeping it in contact with thermoelectric cooler (thermoelectric modules in contact with heat sink). 143 The column contains a control board for electrical control and a temperature sensor. As above, the column is thermally isolated. As opposed to resistive heating, this device can be used for starting the temperature ramp at subambient temperatures.

# ■ MICROFABRICATED PRECONCENTRATORS (μPCS)

Preconcentration is often essential before introducing a sample into the column. The process is used to purify a sample as well as to increase the concentration of the desired analytes in a range that can be detected by the detector used in the GC. PCs are very useful if the concentrations of analytes are in the low parts-perbillion range. The analytes are first collected by passing the sample mixture through a PC over a period of time. The PC is then rapidly heated to inject the analytes into the column as a narrow plug. In a conventional GC system, the PC is typically a small stainless steel or glass tube packed with an adsorbent. These devices have large dead volumes, slow heating rates, and low heating efficiency. 144–147 The microfabricated PC that is ideal for integration with microanalytical systems was first developed by the researchers at SNL. 144 The device comprised a micro hot plate, the surface of which was coated with a surfactant templated sol gel adsorbent. The device was used for the preconcentation of dimethyl methyl phosphonate (DMMP) in the presence of xylene and methyl ethyl ketone as interference. Preconcentration factors as high as 500 and selectivities more than 25 have been obtained. The low heat capacity of the micro hot plate allowed for rapid desorption of the analytes. While the working principle of the PCs is the same, several design modifications have been proposed over the years. SNL later developed three-dimensional  $\mu PC$  in order to increase the surface area that permitted improved analyte collection and concentration.145

The Zellers group at University of Michigan has designed  $\mu$ PCs with increased adsorption capacity and desorption efficiency. <sup>146</sup> A PC not only enhances the concentration but also produces narrowly focused injection plugs due to rapid thermal desorption, and therefore it is also referred to as preconcetrator-focuser (PCF) or preconcentrator-injector

(PCI).  $^{146-149}\mathrm{The}~\mu\mathrm{PCF}$  developed by the Zellers group comprised a silicon microheater with an array of vertically oriented high-aspect-ratio silicon slats as heating elements and the granules of Carbopack X as the adsorbent material. The whole structure was sandwiched between two Pyrex glass plates. A preconcentration factor of approximately 5600 has been achieved for benzene. The group subsequently reported a threestage  $\mu$ PCF to capture vapor spanning a wide range of vapor pressure (4 orders of magnitude). Three different adsorbent materials, including granules of Carbopack B, Carbopack X, and Carboxen 1000, were used. The µPCF showed substantial improvement in performance compared to the previously reported single-stage  $\mu$ PCF. Our group has developed a  $\mu$ PC containing high-aspect-ratio microposts embedded inside an etched silicon cavity. 9,150,151 A thin film of Tenax TA was used as an adsorbent. The structure was sealed by anodically bonding it with to a Pyrex glass wafer. Patterned Cr/Ni stack deposited on the backside (silicon surface) of the device served as heaters and temperature sensors. Dow and Lang<sup>152</sup> designed a  $\mu$ PC comprising 16 silicon microchannels filled with granules of Carboxen 1000. The channels were sealed with Pyrex glass substrate, and Ti/Pt was deposited on the silicon surface to serve as a heater.

In order to generate and control fluid flow through a  $\mu$ GC system, gas valves and pumps are required. A passive  $\mu$ PCI has been recently reported, and this device does not require a pump during the preconcentration step, thereby reducing the power consumption. <sup>153</sup> However, a pump is required to transport the analytes through the downstream components following desorption. In order to reduce the cost and complexity, valveless  $\mu$ GC systems have been developed using a bidirectional Knudsen pump. <sup>10,136</sup>

# DETECTORS

The stream of gas coming from the column is passed through a detector, and the signal obtained as a function of time is used for qualitative and/or quantitative analysis of different components of a mixture. The basic principles of various microdetectors used in a  $\mu GC$  system is briefly discussed in this section.

Thermal Conductivity Detector (TCD). TCD is one of the most widely used detectors in gas analysis. In a TCD, the columns effluent is passed through a sample cell and a stream of pure carrier gas is passed through a reference cell. These cells are equipped with temperature-sensing elements, such as electrically heated metal filament or thermistor. TCDs detect the difference in thermal conductivity between these two streams of gases. Typically, the thermal conductivity of a mixture of carrier gas and solute is lower than that of the pure carrier gas. Hence, when an analyte arrives in the sample channel, a change in signal is observed. Miniaturized TCDs ( $\mu$ TCDs) have been developed by silicon micromachining for use in  $\mu$ GC systems. Heating element constitutes a thin metal film deposited on the surfaces or suspended in microchannels.  $^{9,17,53,70,154}$  The  $\mu$ TCDs, with a subparts per million (subppm) detection limit, are an order of magnitude more sensitive than the conventional TCDs. 53,154 The  $\mu$ TCDs can be separately fabricated or be monolithically integrated with a microcolumn.<sup>9,53</sup>

**Surface Acoustic Wave (SAW) Device.** The operating principle of SAW sensors, which are widely used in gas sensing application, is based on the changes in propagation characteristics of acoustic waves near the surface of a piezoelectric material such as quartz. Williams and Pappas 155 reported a portable GC system incorporating a single SAW sensor. SNL

developed an integrated SAW microsensor array containing four sensors (one reference and three coated sensors) and used the device as a detector in a hand-held gas chromatography system. The array has been used to detect ppm levels of compounds. An important feature of the integrated SAW sensor array is that the response pattern from the array can be combined with the retention time to identify fully resolved and coeluting components of a mixture. A commercial system that uses a single SAW detector is the zNose system by Electronic Sensor Technology. Sensor Technology.

**Chemiresistor Array.** The Zellers group developed a chemiresistor array by depositing gold—thiolate monolayer-protected nanoclusters (MPNs) onto patterned microelectrodes and used this array as a GC detector. The absorption of vapor molecules by the nanoclusters leads to a change in the resistance. The selectivity of the individual sensors in the array has been altered by changing the chemical identity of the monolayer. The initial chemiresistor array comprised two sensors, but later the group used chemiresistor array comprising four sensors. 16,68,141 A chemiresistor typically yields much lower detection limit compared to a SAW sensor.

Chemicapacitive Sensor Array. A capacitive chemical sensor comprises two parallel electrodes or interdigitated electrodes. A sensing material, usually a polymer film, is either sandwiched between the pair of parallel electrodes or coated on the interdigitated electrodes. The absorption of chemical vapors leads to a swelling of polymer and change in electrical permittivity, resulting in a change in the capacitance of the sensor as a function of analyte concentration.  $^{10,159}$  Qin and Gianchandani  $^{10}$  recently reported a dual-chemipacacitive array as a detector in their integrated  $\mu$ GC system.

Nanocantilever. A nanocantilever comprises a beam structure (resonator) that is supported on a rigid support. The resonator is coated with a sensing material (e.g., polymer) and the absorption of gaseous species leads to a change in the resonance frequency proportional to the amount of mass absorbed. Nanocantilevers are fabricated using nanoelectromechanical system (NEMS) technology. These sensors are highly sensitive and have shown a detection limit of subparts per billion. NEMS cantilevers can be used as a single-sensor detector or multisensor detector in a  $\mu$ GC.

Photonionization Detector (PID). A PID comprises a photon source of short-wavelength UV lamp and a small ionization chamber containing the gas sample. The ionization chamber is continuously irradiated with the UV light through an optically transparent window. The energy of the photons depends on the type of gas used in the lamp and the window material. The ionization chamber, whose typical volume is 40-200  $\mu$ L, contains a pair of electrodes. When the energy of a photon is greater than the ionization energy of a molecule, the absorption of the photon results in the ionization of the molecule. The electrodes collect the ions and electrons, and the resulting current varies as a function of the gas concentration. Typically, PIDs are more sensitive than FIDs. 32 While PIDs have been in use as a GC detector for more than 4 decades, recent efforts include the miniaturization of these devices by reducing the volume of the ionization chamber. Sun et al. 161 recently develop a µPID with a lower background noise and faster response time with a detection limit of less than 5 ppb. The volume of the ionization chamber was reduced to 10  $\mu$ L. Zhu et al. 162 have recently developed a flow-through  $\mu$ PID with the chamber volume of 1.3  $\mu$ L with a picogram level detection limit, which is almost 200 times lower than that for commercial PIDs.

This flow-through PID has been used as a detector in portable gas chromatography systems. <sup>11,12</sup> Recently, our group has developed a microhelium discharge photoionization detector using a high-voltage direct current (dc) discharge using a pair of electrodes. <sup>119,163</sup> The detector require auxiliary helium, and as low as 10 pg of octane vapor can be detected. <sup>119</sup> Recently, the Fan group <sup>164</sup> developed miniaturized helium dielectric barrier discharge PID with a detection limit of a few picograms. One of the benefits of these later two devices is that they can be used for ionization of molecules having ionization energy more than 11.8 eV, a range that is not covered by the UV lamps.

Flame Ionization Detector (FID). The FID is one of the most commonly used detectors in GC. The detector is sensitive to those molecules that ionize in a hydrogen—air flame. The charged particles are collected by a collector electrode, thereby generating a minute current. The conventional FID requires large flow of fuel and oxidant; hence, there has been several attempts to develop miniature FIDs. 165–168 However, micro FIDs are less preferred in portable gas chromatography because they require an external source of hydrogen and oxidant.

Electron Capture Detector (ECD). The ECD is a highly sensitive and selective detector for compounds that capture electrons. It is particularly useful for the detection of halogenated, nitroaromatic, organometallic, and conjugated compounds. <sup>169</sup> The ECD contains a source of electrons (e.g., <sup>63</sup>Ni which emits beta electrons) and two polarized electrodes. The beta electrons collide with the molecules of carrier gas to produce a large number of thermal (low energy) electrons, and these electrons produce a reference current. When the column effluent containing high electron affinity atoms enters the detection region, the free electrons are captured by the molecules to form negatively charged ions, resulting in a decrease in current. The originally designed ECD has larger flow cell. The recent development has been in the miniaturization of these devices. Klee et al. 170 described the development of a  $\mu$ ECD with cell volume of 1/10 of the original design with improved sensitivity, larger dynamic range, and much smaller cell volume. These commercialized  $\mu ECDs$  have been used in the analysis of a wide range of samples (reviewed in ref 171). The  $\mu$ ECDs are amenable for a  $\mu$ GC system.

lon Mobility Spectrometer (IMS). The IMS has been widely used as a detector in gas chromatography. The working principle of IMS is based on the differential migration of ions in an electric field in the presence of an inert gas. The most common source of ionization is beta electrons from a small foil of radioactive <sup>63</sup>Ni. A variant of IMS that has been miniaturized and amenable for portable GC is differential mobility spectrometer (DMS). <sup>172–174</sup> The DMS comprises two parallel planar electrodes separated by a narrow gap where ions are transported by a gas flow and a high-voltage radio frequency asymmetric waveform applied perpendicular to the direction of ion transport. At low electric fields, the ion mobility is field independent, while the mobility becomes field-dependent at high electric fields. The field oscillates between low and high fields, resulting in the separation of ions that are collected by a pair of biased electrodes.

# ■ BRIEF HISTORY AND CURRENT STATUS OF MICRO GC

The concept of chip-scale GC was introduced by Terry, Jerman, and Angell from Stanford University in 1979.<sup>70</sup> In their pioneering work, the authors developed a miniature GC system

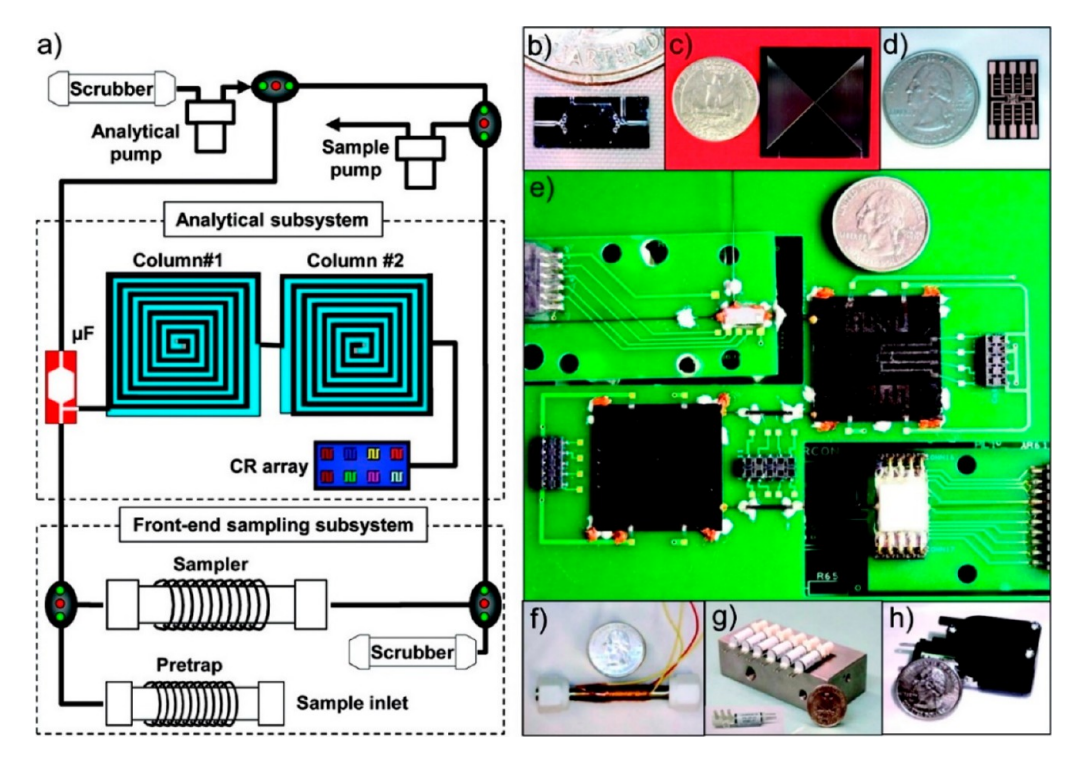


Figure 9. A  $\mu$ GC prototype developed by the Zellers group: (a) schematic of fluidic pathways and (b-h) photographs of major components (b) microfocuser, (c) 3 m long microcolumn, (d) four-chemiresistor array detector, (e) integrated system, (f) sampler/pretrap, (g) valve and valve manifold, and (h) miniature diaphragm pump. Reproduced with permission from ref 141. Copyright 2011 American Chemical Society.

by fabricating a sample injection valve and a 1.5 m long spiral separation column (roughly rectangular in cross section) both fabricated on a 2 in. silicon wafer. The silicon wafer was anodically bonded with a Pyrex cover plate to prepare an enclosed chromatographic column. The column was first treated with an organosilane compound. Subsequently, a standard stationary phase (e.g., OV-101) dissolved in a volatile solvent was forced through the column to prepare a film of the stationary phase. A miniature TCD was separately batch fabricated and mounted on the same silicon wafer. The separation was very fast; however, the resolving power of the column was less compared to the standard column of that time mainly because of the limitations in obtaining uniform stationary phase coating.

Subsequent studies by Kolesar and Reston 60,116 in the early 1990s were directed toward addressing Terry's limitation by focusing in the production of a more homogeneous stationary phase film. The authors fabricated a miniature GC using silicon micromachining and integrated circuit processing techniques. The miniature GC comprised a miniature sample injector, 0.9 m long rectangular cross section (300  $\mu$ m × 10  $\mu$ m) spiral column and dual detector scheme (chemiresistor and thermal conductivity detector bead). The authors were able to deposit a nearly homogeneous thin film (200 nm thick) of copper phthalocyanine onto the surfaces of the etched channels through sublimation prior to anodic bonding of the silicon wafer with borosilicate glass plate. The authors employed the miniature GC for isothermal separation of ammonia and nitrogen dioxide at parts-per-million levels in less than 30 min. More intensive studies to develop integrated  $\mu$ GC systems were conducted by the researchers at SNL and UM. SNL made significant efforts in the development of microanalytical systems by initiating a "MicroChemLab" program in 1996. 175 The initial motivation of this program was to develop battery-operated hand-held microsystems for sensitive and selective detection of chemical

warfare agents; nonetheless, the range of analytes has been later expanded to encompass other mixtures, including explosives, petrochemicals, trihalomethanes, toxic industrial chemicals, and fatty acid methyl esters. <sup>175,176</sup> The  $\mu$ GC system, named as the "µChemLab", comprised three major components: microfabricated sample preconcentrator, 1 m long microfabricated spiral column on a 1.0-1.5 cm<sup>2</sup> silicon chip, and a miniaturized SAW array detector.<sup>69</sup> These three components were serially connected to develop a dual channel system providing desired sensitivity and selectivity. The preconcentrator allowed for selectively collecting and concentrating an analyte. Moreover, the use of a SAW sensor array, with each sensor element coated with a different chemical, allowed the identification of analytes by generating distinct response patterns. By placing selective coatings on each of the devices, improvement in selectivity and reduction in false positives of the overall system can be achieved.<sup>175</sup> Detection limits as low as subparts per billion concentration level has been achieved using  $\mu$ ChemLab. <sup>177</sup> SNL also developed and patented temperature programmable microfabricated columns by incorporating resistive heating element and temperature sensors.

The efforts at the Wireless Integrated MicroSystems (WIMS) National Science Foundation Engineering Research Center (NSF-ERC) led by Dr. Wise at UM had a profound impact on moving the technology forward from preconcentratons to separation columns and detectors in addition to integration of these MEMS-enabled components to realize portable GCs. One of the  $\mu$ GCs reported by Lu et al. <sup>68</sup> incorporates all essential analytical components, including a sample inlet with particulate filter, on-board calibration-vapor source, a multistage preconcentrator-focuser, a separation column, integrated four-chemiresistor sensor array detector, pump, and valves. The column comprised a 3 m long square-spiral channel dynamically coated with PDMS. This system was used for temperature-programmed

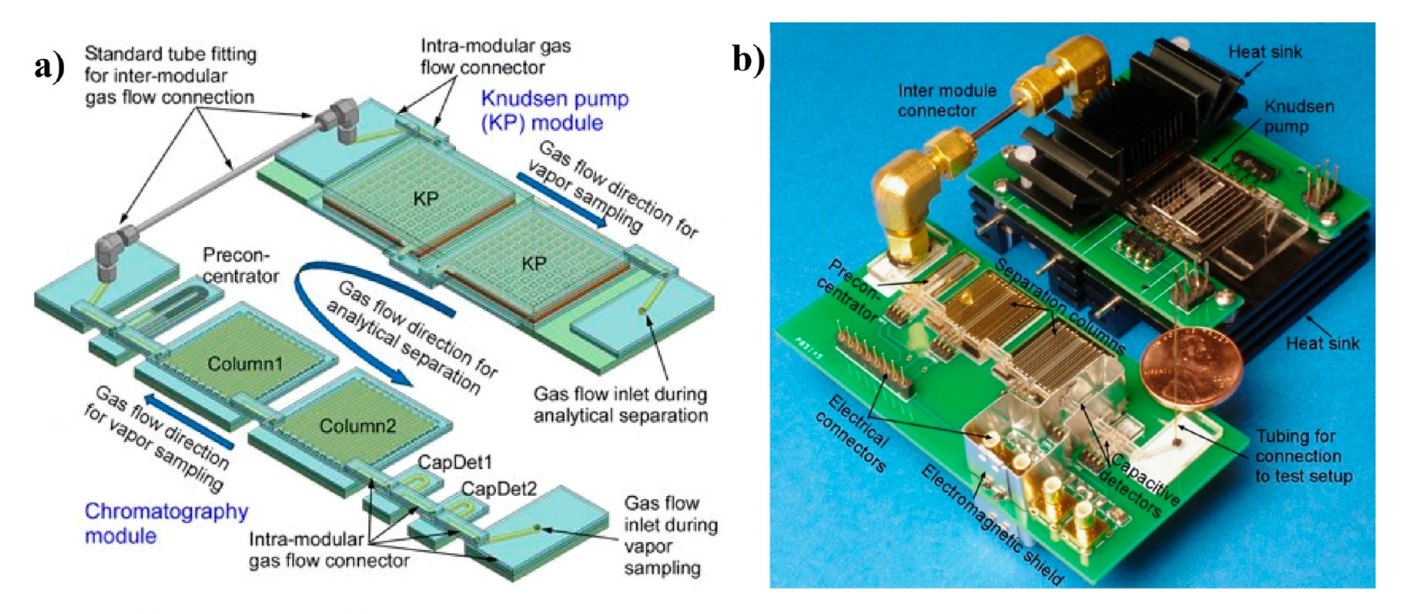
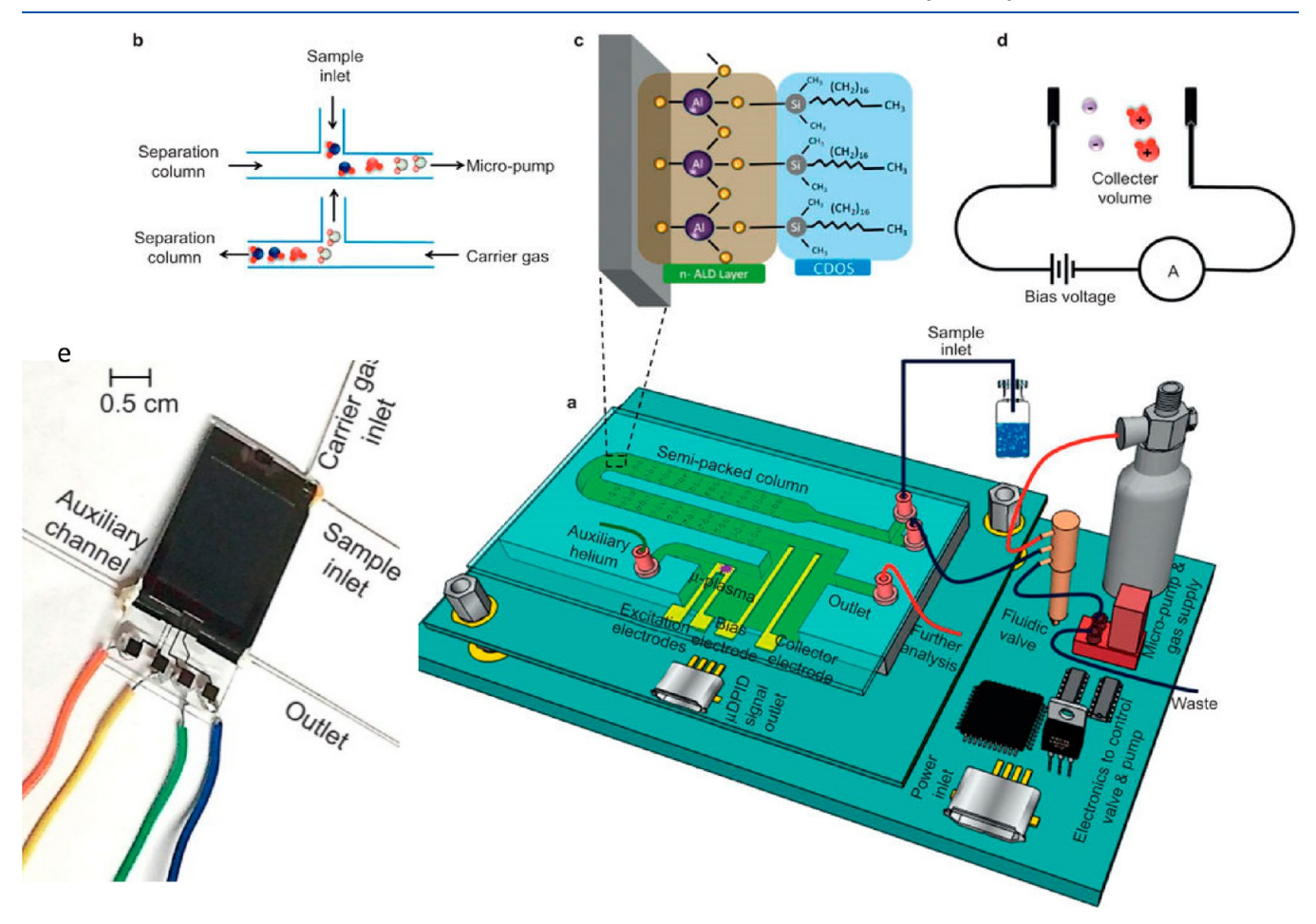


Figure 10. (a) Block diagram and (b) photograph of a  $\mu$ GC system developed by Qin and Gianchandani. To visualize the inner structure, one of the heat sinks of Knudsen pump has been removed in part b. Modified and reproduced from ref 10. Copyright Springer Nature.



**Figure 11.** Block diagram of the chip-scale GC platform developed by VT MEMS Lab: (a) setup displaying the fluidic interconnections between the chip, valve, micropump, and carrier gas, (b) injection mechanism with the top image showing the loading phase and the bottom image showing the injection phase, (c) coating mechanism for SPC, (d) electrical circuit for measuring current signal, and (e) an optical image of the packaged chip. Reproduced from ref 107. Copyright Springer Nature.

separation of a mixture of 11 compounds in less than 90 s with projected detection limits in the range of low (5-130) parts per billion using ambient air as the carrier gas. A combination of

retention time and the sensor-array response pattern was used to uniquely identify each of the 11 compounds. Since then, there has been significant progress in the development of individual

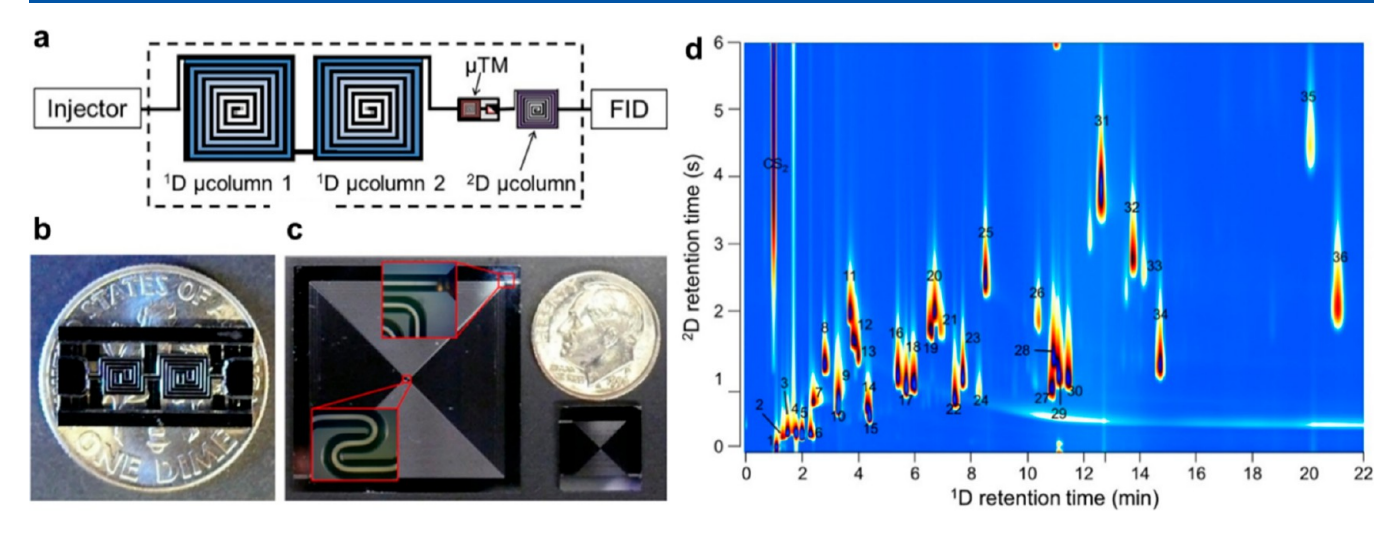


Figure 12. The  $\mu$ GC ×  $\mu$ GC system developed by the Zellers team: (a) block diagram of the experimental setup with the dashed box showing the benchtop GC oven, (b)  $\mu$ TM on a U.S. dime, (c) 3 m long  $^1$ D column (on the left of dime), 0.5 m long  $^2$ D column (below dime), and the insets showing the magnified view of selected regions of  $^1$ D column, and (d) a 2D contour plot showing the separation of a 36-component mixture comprising both polar and nonpolar compounds using the microsystem. Reproduced with permission from ref 47. Copyright 2015 American Chemical Society.

components as well as integration of these components for analysis of complex mixtures of volatile organic compounds (VOCs).  $^{10,141,148,149,178-180}$ 

Figure 9 shows a field-deployable  $\mu$ GC system developed by the Zellers group. <sup>141</sup> This  $\mu$ GC was adapted for the analysis of low-level trichloroethylene (TCE) vapors in air. The generation and control of fluidic flow through the  $\mu$ GC was achieved using a set of valves and pumps. In order to reduce analysis time and detection limit, a pretrap and high-volume sampler made of thinwalled stainless steel tubes were used. The pretrap packed with Carbopack B was used for capturing interfering compounds with vapor pressure  $(p_v)$  less than 3 Torr, while the Carbopack Xpacked sampler was used for capture of compounds with  $p_y$ within a range of 3–95 Torr ( $p_v$  of TCE is 69 Torr). Coils of insulated copper wires were used to heat both the pretrap and sampler. The captured TCE and other compounds were then transferred to a focuser, which was comprised of an etched silicon bonded to Pyrex glass with integrated resistive heaters. The microfocuser was packed with Carbopack X. The captured compounds were rapidly heated to inject them to the separation module as a narrow plug. The separation module was comprised of two series-coupled silicon-glass microcolumns with integrated resistive heaters. Each column has a length of 3 m and coated with PDMS stationary phase with temperature programming capabilities. The detector consisted of a four-chemiresistor sensor array. The array chip was comprised of 8 Au/Cr interdigitate electrodes in a  $4 \times 2$  pattern on a SiO<sub>x</sub>/Si substrate. The chip was coated with four types of MPNs (i.e., two sensors were coated with each MPN). The  $\mu$ GC was used for recognition and quantification of TCE in the presence of up to 45 interfering compounds. The collection of 20 L sample required 26 min with a preconcentrator factor of 500 000 and a detection limit of 40 parts per trillion (ppt).

Figure 10 shows a block diagram and photograph of a  $\mu$ GC system developed by Qin and Gianchandani<sup>10</sup> at University of Michigan. The  $\mu$ GC system, with all the components microfabricated, comprised a bidirectional Knudsen pump, a two-stage preconcentrator, two separation columns, and two complementary capacitive detectors. The Knudsen pump, which does not require any moving parts, operates on the

principle of thermal transpiration, a thermal-gradient induced movement of gas molecules from the cold end toward the hot end of a channel. The use of bidirectional pump obviates the need for valves, thereby reducing the complexity. The capacitive detectors has closely spaced interdigitate electrodes coated with a layer of OV-1; the polymer thickness was kept different for the two detectors. The absorption of vapors results in swelling as well as change in electrical permittivity of the polymer, thereby changing the capacitance. The two detectors provided complementary responses, which were useful for enhanced vapor recognition and resolution of coeluting peaks. The system was used for the separation of 19 chemicals with a detection limit as low as 2 parts per billion.

Virginia Tech MEMS Laboratory has also played a crucial role not only in creating new MEMS-enabled  $\mu$ GC separation columns and stationary phases but also in monolithic integration of these columns with different microfabricated detectors including TCDs and micro helium-discharge photoionization detectors ( $\mu$ PIDs). Pigure 11 shows a chip-scale gas chromatography system comprising the key components, including a sample injection unit, SPC, and  $\mu$ PID developed by our group. These GC-on-chip alleviate the external transfer lines between the column and detector and prevent the formation of cold spots and the variation in the cross-sectional areas through which the gas traverses, thereby, suppressing band broadening and improving overall chromatographic separation. These unique chips also provide the ability to perform multidimensional separations and to realize a GC Matrix. 181,182

In the past decade, several research groups have shifted their efforts toward the development of fast 2D GC using either MEMS columns or short capillary columns.  $^{12,14,26,47,11,183,184}$  While the first GC  $\times$  GC was reported by Liu and Phillips in 1991,  $^{45}$  the first GC  $\times$  GC using microfabricated components was developed by Whiting and co-workers at SNL and Caltech in 2009.  $^{111}$  This 2D GC system was composed of two microfabricated columns with spiral geometry and nanoelectromechanical systems (NEMS)-based cantilevers coated with a polymeric film as a sensitive detector. The first-dimension 90 cm long and the second-dimension 30 cm long columns were coated with a relatively nonpolar PDMS and a polar PEG

stationary phases, respectively. By using pneumatic modulation, the authors were able to separate dimethyl methylphosphonate (DMMP), a nerve agent surrogate, from three polar interfering compounds in just a few seconds.

Subsequently, the Zellers team made notable contributions in the field of 2D  $\mu$ GC. <sup>47,183</sup> The initial effort of the team was the development and evaluation of a liquid cryogen-free microfabricated thermal modulator ( $\mu$ TM). <sup>142,185</sup> Thermal modulators typically provide higher sensitivity enhancement as compared to pneumatic modulators. The  $\mu$ TM was fabricated using two series-coupled Pyrex-on-silicon microchannels, which were coated with PDMS. The device was sequentially cooled and heated to trap and desorb the analytes. The unique advantages of this  $\mu$ TM are (i) it consumes at least 2 orders of magnitude less power than a conventional TM and (ii) it does not require any cryogenic fluids for cooling. This  $\mu$ TM was later employed in  $\mu GC \times \mu GC^{47,183}$  as well as benchtop GC  $\times$  GC systems. <sup>186,187</sup> Figure 12a–c shows a  $\mu$ GC  $\times$   $\mu$ GC system developed by the Zellers team. 47 The authors used 3 m long 1D microcolumn coated with OV-1 and 0.5 m long <sup>2</sup>D microcolumn coated with OV-215 for a successful separation of a 36component mixture comprising different classes of polar and nonpolar compounds spanning a wide range of boiling points (Figure 12d). While the authors utilized a conventional GC oven, injector, and detector in the current studies, this a significant step toward the development of fully integrated  $\mu$ GC  $\times \mu GC$  systems.

While 2D GC is a promising technology, significant instrumental challenges are associated with achieving the theoretical maximum peak capacity. Fan and co-workers 12,14,26,184 at University of Michigan have also been working to further enhance the separation performance of 2D  $\mu$ GCs. Recently, the team proposed a new concept of "adaptive" or "smart multichannel" two-dimensional (micro) GC. The system comprises a single <sup>1</sup>D capillary (conventional) column, multiple parallel <sup>2</sup>D (conventional) columns, and a "decision-making module" between <sup>1</sup>D and <sup>2</sup>D columns. The decision-making module comprised a nondestructive on-column detector (i.e., micro photoionization detector) and a flow-routing system. The flow-routing system, which is activated by the first detector, comprised multiport valves and thermal modulators (low frequency), and this system directs the effluents from the <sup>1</sup>D column to one of the <sup>2</sup>D columns for further separation. A schematic illustration of the adaptive 2D (micro) GC is shown in Figure 13. There are several advantages of the adaptive 2D GC: (1) The system delivers an increase in peak capacity,

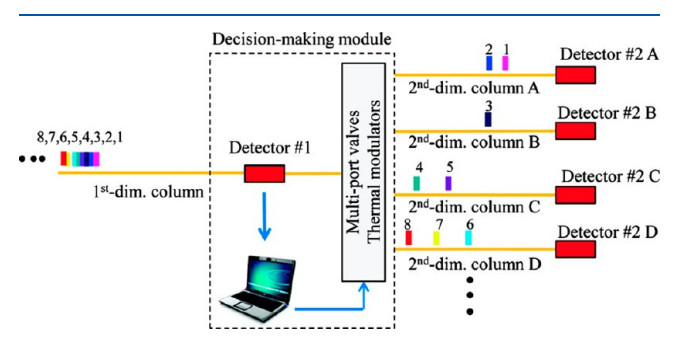


**Figure 13.** Schematic illustration of the design concept of an adaptive two-dimensional (micro) gas chromatography system proposed by the Fan group. Reproduced with permission from ref 26. Copyright 2012 American Chemical Society.

because modulation causes a peak broadening of the first dimension due to resampling and subsequent reconstruction of the peaks; <sup>188,189</sup> (2) there is no constraint in the length of the <sup>2</sup>D column, thereby increasing the overall peak capacity; <sup>189</sup> (3) the elimination of high-frequency thermal modulator lowers the power consumption; and (4) the system simplifies complex postprocessing of data. The group has recently developed a fully portable adaptive 2D GC and employed the system to detect multiple VOCs in an occupational setting. <sup>12,14</sup> While being a promising technology, the authors point out some limitations, which include increased dead volume and the requirement of more sensitive first detector to activate the flow-routing system. <sup>26</sup>

#### RECOMMENDATIONS

Considerable efforts in  $\mu$ GCs are centered on the development of microcolumns; however, a direct comparison of column performance is challenging due to several limitations. One of the most widely used metrics to assess the column quality is the separation efficiency, which is expressed in plate numbers per meter or plate height. The column efficiency of a microcolumn depends on a number of parameters including the geometry of the column; width of the channels; thickness, uniformity, and the type of the stationary phase; retention factor; identity of the test compound; and carrier gas and its velocity. Useful guidelines to evaluate the quality of capillary columns have been provided by Poole and Lenca.<sup>35</sup> Similar procedures should be followed for microcolumn characterization. The authors have recommended that the test compound used to evaluate column efficiency should exhibit good solubility in the stationary phase and should be well retained with a retention factor greater than 5.35 Compared to a well-retained compound, unretained and weakly retained compounds can show unusually high plate numbers which obviously cannot represent the column performance.<sup>48</sup> Plate numbers should be determined under isothermal conditions. While there are some reports where plate numbers have been determined under temperature-programmed conditions, <sup>101</sup> these values are highly inflated (we have observed up to 20-fold enhancement) and should never be compared with the values obtained under isothermal conditions. When comparing the plate numbers of two sets of columns, a significant test should be carried out before making any conclusion. Another quality metric is the tailing factor. Peak tailing is due to surface activity which reduces the sensitivity particularly for polar analytes. The surface activity can be minimized by deactivating the surface using different agents.<sup>81</sup> To assess the surface activity of capillary columns, a mixture of test probes containing both polar and nonpolar compounds have been recommended by different investigators including Grob et al. 190 and Luong et al. 191 Similar mixtures should be used to evaluate the activity of microcolumns.

In microcolumns, connecting capillary tubings are used for gas transfer to and from the column. The contribution of the coated connecting capillary needs to be taken into account while calculating the number of theoretical plates. <sup>47</sup> If these columns are used within a  $\mu$ GC platform, then the length of the connecting capillaries is likely to be 1–2% of the overall length of the column and their contribution can be neglected. However, if these MEMS columns are tested in GC ovens, such as an Agilent 7890A, then the plate number needs to be readjusted to take into consideration the effect of the coated capillary tubing. However, one should not simply calculate the plate number of the  $\mu$ GC column through length ratios as this does not accurately reflect

the MEMS column performance due to inherent differences between the two columns.

Another factor to consider is the footprint of the column. Decreasing the footprint of a column reduces the manufacturing costs and power consumption. Minimizing power consumption has been one of the key objectives in realizing field-portable  $\mu$ GCs. <sup>109</sup> In fact, it is important to notice that the efficiency of conventional GC columns are characterized based on unit length as the length of the column determines the cost. Microfabricated columns, however, are implemented on planar substrates using similar technologies used to manufacture microelectronic chips. Therefore, the cost is related to the total area of the chip. This means that a new metric should be generated for MEMS columns to reflect this significant attribute while providing meaningful chromatographic performance. One proposed new metric is to report the number of theoretical plates per unit area and not per unit length. This new metric takes into consideration the delicate care in the design of such columns to improve efficiency in a very small area by full utilization of MEMS design and fabrication. An additional important parameter that should be reported is the pressure drop (per unit length) across the column at the optimal carrier gas flow velocity as this can have an influence on the size and the power of the mini-pump to deliver the required pressure. Other considerations include sample capacity, peak capacity, and temperature operating range, which are important for gas chromatographic analysis.

# **■ CONCLUSIONS AND PERSPECTIVE**

Interest in portable GC instruments is rapidly increasing due to the desire for rapid and on-site analysis of environmental, food, agricultural, pharmaceutical, and forensic samples. Micro GC has undergone significant transformation in different aspects, including chromatographic theory, preconcentrators/injectors, separation columns, stationary phases, and detectors since its introduction by Terry in 1979. Numerous manufacturers have currently commercialized portable GCs comprising one or several microfabricated components, and there have been ongoing efforts in the development of more efficient micro GC systems for the analysis of more complex samples. Significant advancements have been achieved in the development of new stationary phases. Advancements in semipacked (pillar array) and multicapillary columns have contributed in increased separation efficiency, peak capacity, and sample capacity. Similarly, advancement in multidimensional µGCs have been very promising in enhancing the peak capacity and the ability to separate complex mixtures spanning a wide range of analyte polarity.

One point of consideration is that  $\mu$ GC columns have been tested with a limited number of test mixtures under laboratory conditions. The majority of the studies are focused on the separation of simple hydrocarbons, and at the same time, significantly distorted peaks have been observed. <sup>57,63,72,101</sup> MEMS GCs has potential to analyze much wider range of analytes. The future research could be focused on the development of even more efficient and lower power separation columns, efficient deactivation protocols, versatile and effective stationary phase materials, and wearable  $\mu$ GCs.

#### ASSOCIATED CONTENT

# S Supporting Information

The Supporting Information is available free of charge on the ACS Publications website at DOI: 10.1021/acs.analchem.8b01461.

Basic concepts and terms of GC and a short list of commercially available portable GC systems (PDF)

#### AUTHOR INFORMATION

#### **Corresponding Authors**

\*E-mail: bishnu7@vt.edu. \*E-mail: agah@vt.edu.

#### ORCID

Bishnu P. Regmi: 0000-0001-7690-9825

#### Notes

The authors declare the following competing financial interest(s): Masoud Agah is a co-founder and the Chief Technology Officer of Zebra Anlytix, Inc. Masoud Agah and Bishnu Regmi are co-authors of patent applications licensed to Zebra Analytix, Inc. through Virginia Tech Intellectual Properties

#### **Biographies**

Bishnu Regmi obtained his Ph.D. degree in Analytical Chemistry from Louisiana State University in 2014. His research interests primarily focus on the applications of ionic liquids in sensing and separations. He did 2 years of postdoctoral studies at Virginia Tech where he developed ionic liquid-coated microcolumns for the separation of a range of mixtures. Currently, he is teaching at Grossmont College (El Cajon, CA) and Southwestern College (Chula Vista, CA).

Masoud Agah obtained his Ph.D. degree in Electrical Engineering from the University of Michigan in 2005. He joined the faculty at Virginia Tech in 2005, where he is currently the Virginia Microelectronics Consortium Professor of Engineering in the Bradley Department of Electrical and Computer Engineering. He established the VT MEMS Laboratory in 2005 and has focused his research on environmental and biomedical applications of MEMS and microfluidics. He received the National Science Foundation CAREER Award in 2008 for his research on micro gas chromatography.

#### ACKNOWLEDGMENTS

The work was supported by the Bradley Department of Electrical and Computer Engineering and the National Science Foundation under Award ECCS-1711699.

# REFERENCES

- (1) Kotiaho, T. J. Mass Spectrom. 1996, 31, 1-15.
- (2) Lopez-Avila, V.; Hill, H. H. Anal. Chem. 1997, 69, 289-306.
- (3) Giannoukos, S.; Brkić, B.; Taylor, S.; Marshall, A.; Verbeck, G. F. Chem. Rev. **2016**, 116, 8146–8172.
- (4) Hinshaw, J. V.; Advanstar Communications 131 W. First St., Duluth, MN 55802. USA, 2003.
- (5) Lu, C.-J.; Whiting, J.; Sacks, R. D.; Zellers, E. T. Anal. Chem. 2003, 75, 1400–1409.
- (6) Contreras, J. A.; Murray, J. A.; Tolley, S. E.; Oliphant, J. L.; Tolley, H. D.; Lammert, S. A.; Lee, E. D.; Later, D. W.; Lee, M. L. *J. Am. Soc. Mass Spectrom.* **2008**, *19*, 1425–1434.
- (7) Bednar, A. J.; Russell, A. L.; Georgian, T.; Splichal, D.; Hayes, C. A.; Tackett, P.; Jones, W. T.; Justes, D.; Parker, L.; Kirgan, R. A. Field-Portable Gas Chromatograph Mass Spectrometer (GC-MS) Unit for Semi-Volatile Compound Analysis in Groundwater; Engineer Research and Development Center Vicksburg MS Environmental Lab, 2011.

- (8) Yu, C. M. High Performance Hand-Held Gas Chromatograph; Lawrence Livermore National Laboratory: Livermore, CA, 1998.
- (9) Garg, A.; Akbar, M.; Vejerano, E.; Narayanan, S.; Nazhandali, L.; Marr, L. C.; Agah, M. Sens. Actuators, B **2015**, 212, 145–154.
- (10) Qin, Y.; Gianchandani, Y. B. Microsyst. Nanoeng. 2016, 2, 15049.
- (11) Zhou, M.; Lee, J.; Zhu, H.; Nidetz, R.; Kurabayashi, K.; Fan, X. RSC Adv. 2016, 6, 49416–49424.
- (12) Lee, J.; Zhou, M.; Zhu, H.; Nidetz, R.; Kurabayashi, K.; Fan, X. Anal. Chem. **2016**, 88, 10266–10274.
- (13) Tzeng, T.-H.; Kuo, C.-Y.; Wang, S.-Y.; Huang, P.-K.; Huang, Y.-M.; Hsieh, W.-C.; Huang, Y.-J.; Kuo, P.-H.; Yu, S.-A.; Lee, S.-C. *IEEE J. Solid-State Circuits* **2016**, *51*, 259–272.
- (14) Lee, J.; Sayler, S. K.; Zhou, M.; Zhu, H.; Richardson, R. J.; Neitzel, R. L.; Kurabayashi, K.; Fan, X. Anal. Methods 2018, 10, 237.
- (15) Zampolli, S.; Elmi, I.; Mancarella, F.; Betti, P.; Dalcanale, E.; Cardinali, G.; Severi, M. Sens. Actuators, B 2009, 141, 322–328.
- (16) Wang, J.; Bryant-Genevier, J.; Nuñovero, N.; Zhang, C.; Kraay, B.; Zhan, C.; Scholten, K.; Nidetz, R.; Buggaveeti, S.; Zellers, E. T. *Microsyst. Nanoeng.* **2018**, *4*, 17101.
- (17) Dziuban, J.; Mroz, J.; Szczygielska, M.; Małachowski, M.; Gorecka-Drzazga, A.; Walczak, R.; Buła, W.; Zalewski, D.; Łysko, J.; Koszur, J. Sens. Actuators, A 2004, 115, 318–330.
- (18) Manginell, R. P.; Bauer, J. M.; Moorman, M. W.; Sanchez, L. J.; Anderson, J. M.; Whiting, J. J.; Porter, D. A.; Copic, D.; Achyuthan, K. E. Sensors 2011, 11, 6517–6532.
- (19) Jian, R.-S.; Huang, Y.-S.; Lai, S.-L.; Sung, L.-Y.; Lu, C.-J. Microchem. J. 2013, 108, 161–167.
- (20) INFICON. http://products.inficon.com/en-us/product/detail/micro-gc-fusion-gas-analyzer/ (accessed on March 20, 2018).
- (21) Agilent Technologies. https://www.agilent.com/en/products/gas-chromatography/gcsystems/490-micro-gc-system (accessed on March 20, 2018).
- (22) Apix Analytics. http://www.apixanalytics.com/chrompix/. (accessed on March 20, 2018).
- (23) Defiant Technologies. http://www.defiant-tech.com/frog-4000. php (accessed on March 20, 2018).
- (24) NANOVA Environmental. https://www.nanovaenv.com/novatest-p100/ (accessed on March 20, 2018).
- (25) Lee, J.; Zhou, M.; Zhu, H.; Nidetz, R.; Kurabayashi, K.; Fan, X. *Analyst* **2016**, *141*, 4100–4107.
- (26) Liu, J.; Khaing, O. M. K.; Reddy, K.; Gianchandani, Y. B.; Schultz, J. C.; Appel, H. M.; Fan, X. *Anal. Chem.* **2012**, *84*, 4214–4220.
- (27) Azzouz, I.; Vial, J.; Thiébaut, D.; Haudebourg, R.; Danaie, K.; Sassiat, P.; Breviere, J. Anal. Bioanal. Chem. 2014, 406, 981–994.
- (28) Haghighi, F.; Talebpour, Z.; Sanati-Nezhad, A. Lab Chip 2015, 15, 2559–2575.
- (29) Lussac, E.; Barattin, R.; Cardinael, P.; Agasse, V. Crit. Rev. Anal. Chem. 2016, 46, 455–468.
- (30) Sidelnikov, V. N.; Nikolaeva, O. A.; Platonov, I. A.; Parmon, V. N. Russ. Chem. Rev. **2016**, 85, 1033.
- (31) Wang, A.; Tolley, H. D.; Lee, M. L. J. Chromatogr. A **2012**, 1261, 46–57.
- (32) Poole, C. F. J. Chromatogr. A 2015, 1421, 137-153.
- (33) Voiculescu, I.; Zaghloul, M.; Narasimhan, N. TrAC, Trends Anal. Chem. 2008, 27, 327–343.
- (34) Ghosh, A.; Vilorio, C. R.; Hawkins, A. R.; Lee, M. L. *Talanta* **2018**, *188*, 463–492.
- (35) Poole, C. F.; Lenca, N. J. Chromatogr. A 2014, 1357, 87–109.
- (36) Van Deemter, J. J.; Zuiderweg, F.; Klinkenberg, A. Chem. Eng. Sci. **1956**, *5*, 271–289.
- (37) Golay, M. J. In *Gas Chromatography*; Butterworths: London, 1958; p 36.
- (38) Spangler, G. E. Anal. Chem. 1998, 70, 4805-4816.
- (39) Spangler, G. E. J. Microcolumn Sep. 2001, 13, 285-292.
- (40) Spangler, G. E. Anal. Chem. 2006, 78, 5205-5207.
- (41) Dolan, J. W. LCGC Eur. 2003, 16, 610-613.
- (42) Giddings, J. C. Anal. Chem. 1967, 39, 1027-1028.
- (43) Davis, J. M.; Giddings, J. C. Anal. Chem. 1983, 55, 418-424.
- (44) Giddings, J. C. J. Chromatogr. A 1995, 703, 3–15.

- (45) Liu, Z.; Phillips, J. B. J. Chromatogr. Sci. 1991, 29, 227-231.
- (46) Libardoni, M.; Waite, J. H.; Sacks, R. Anal. Chem. 2005, 77, 2786–2794.
- (47) Collin, W. R.; Bondy, A.; Paul, D.; Kurabayashi, K.; Zellers, E. T. *Anal. Chem.* **2015**, 87, 1630–1637.
- (48) Jespers, S.; Schlautmann, S.; Gardeniers, H. J.; De Malsche, W.; Lynen, F.; Desmet, G. Anal. Chem. **2017**, 89, 11605–11613.
- (49) Ghosh, A.; Johnson, J. E.; Nuss, J. G.; Stark, B. A.; Hawkins, A. R.; Tolley, L. T.; Iverson, B. D.; Tolley, H. D.; Lee, M. L. *J. Chromatogr. A* **2017**, *1517*, 134–141.
- (50) Li, Y.; Zhang, R.; Wang, T.; Wang, Y.; Wang, Y.; Li, L.; Zhao, W.; Wang, X.; Luo, J. *Talanta* **2016**, *154*, 99–108.
- (51) Radadia, A. D.; Morgan, R. D.; Masel, R. I.; Shannon, M. A. Anal. Chem. **2009**, *81*, 3471–3477.
- (52) Matzke, C. M.; Kottenstette, R. J.; Casalnuovo, S. A.; Frye-Mason, G. C.; Hudson, M. L.; Sasaki, D. Y.; Manginell, R. P.; Wong, C. C. *Proc. SPIE* **1998**, *3511*, *262*.
- (53) Kaanta, B. C.; Chen, H.; Zhang, X. J. Micromech. Microeng. 2010, 20, 055016
- (54) Haudebourg, R.; Vial, J.; Thiebaut, D.; Danaie, K.; Breviere, J.; Sassiat, P.; Azzouz, I.; Bourlon, B. Anal. Chem. 2013, 85, 114–120.
- (55) He, B.; Tait, N.; Regnier, F. Anal. Chem. 1998, 70, 3790-3797.
- (56) Wang, A.; Hynynen, S.; Hawkins, A. R.; Tolley, S. E.; Tolley, H. D.; Lee, M. L. *J. Chromatogr. A* **2014**, *1374*, 216–223.
- (57) Nakai, T.; Nishiyama, S.; Shuzo, M.; Delaunay, J.; Yamada, I. J. Micromech. Microeng. 2009, 19, 065032.
- (58) Vial, J.; Thiébaut, D.; Marty, F.; Guibal, P.; Haudebourg, R.; Nachef, K.; Danaie, K.; Bourlon, B. J. Chromatogr. A 2011, 1218, 3262—3266
- (59) Ali, S. In Proceedings of the 11th International Conference on Miniaturized Systems for Chemistry and Life Sciences ( $\mu$ TAS 2007), Paris, France, 2007; Vol. 10, pp 239–241.
- (60) Reston, R. R.; Kolesar, E. J. Microelectromech. Syst. 1994, 3, 134–146.
- (61) Shakeel, H.; Rice, G. W.; Agah, M. Sens. Actuators, B 2014, 203, 641-646.
- (62) Shakeel, H.; Wang, D.; Heflin, J. R.; Agah, M. Sens. Actuators, B **2015**, 216, 349–357.
- (63) Ali, S.; Ashraf-Khorassani, M.; Taylor, L. T.; Agah, M. Sens. Actuators, B 2009, 141, 309-315.
- (64) Bhushan, A.; Yemane, D.; Trudell, D.; Overton, E. B.; Goettert, J. Microsyst. Technol. 2006, 13, 361–368.
- (65) Noh, H.-s.; Hesketh, P. J.; Frye-Mason, G. C. J. Microelectromech. Syst. 2002, 11, 718–725.
- (66) Malainou, A.; Vlachopoulou, M.; Triantafyllopoulou, R.; Tserepi, A.; Chatzandroulis, S. J. Micromech. Microeng. 2008, 18, 105007.
- (67) Rankin, J. M.; Suslick, K. S. Chem. Commun. 2015, 51, 8920–8923.
- (68) Lu, C. J.; Steinecker, W. H.; Tian, W. C.; Oborny, M. C.; Nichols, J. M.; Agah, M.; Potkay, J. A.; Chan, H. K. L.; Driscoll, J.; Sacks, R. D.; Wise, K. D.; Pang, S. W.; Zellers, E. T. *Lab Chip* **2005**, *5*, 1123–1131.
- (69) Frye-Mason, G.; Kottenstette, R.; Lewis, P.; Heller, E.; Manginell, R.; Adkins, D.; Dulleck, G.; Martinez, D.; Sasaki, D.; Mowry, C. In *Micro Total Analysis Systems* 2000; Springer, 2000; pp 229–232.
- (70) Terry, S. C.; Jerman, J. H.; Angell, J. B. *IEEE Trans. Electron Devices* **1979**, *26*, 1880–1886.
- (71) Yuan, H.; Du, X.; Tai, H.; Li, Y.; Zhao, X.; Guo, P.; Yang, X.; Su, Y.; Xiong, Z.; Xu, M. Sens. Actuators, B **2017**, 239, 304–310.
- (72) Gaddes, D.; Westland, J.; Dorman, F. L.; Tadigadapa, S. J. Chromatogr. A 2014, 1349, 96–104.
- (73) Zampolli, S.; Elmi, I.; Stürmann, J.; Nicoletti, S.; Dori, L.; Cardinali, G. Sens. Actuators, B 2005, 105, 400–406.
- (74) Lambertus, G.; Elstro, A.; Sensenig, K.; Potkay, J.; Agah, M.; Scheuering, S.; Wise, K.; Dorman, F.; Sacks, R. *Anal. Chem.* **2004**, *76*, 2629–2637.
- (75) Stadermann, M.; McBrady, A. D.; Dick, B.; Reid, V. R.; Noy, A.; Synovec, R. E.; Bakajin, O. *Anal. Chem.* **2006**, *78*, 5639–5644.

- (76) Radadia, A.; Salehi-Khojin, A.; Masel, R.; Shannon, M. Sens. Actuators, B 2010, 150, 456–464.
- (77) Bhushan, A.; Yemane, D.; McDaniel, S.; Goettert, J.; Murphy, M. C.; Overton, E. B. *Analyst* **2010**, *135*, 2730–2736.
- (78) Cui, Z. In *Encyclopedia of Microfluidics and Nanofluidics*; Springer, 2015; pp 68–73.
- (79) Manginell, R. P.; Frye-Mason, G. C. Temperature Programmable Microfabricated Gas Chromatography Column. U.S. Patent 6,666,907, December 23, 2003.
- (80) Reidy, S.; George, D.; Agah, M.; Sacks, R. Anal. Chem. 2007, 79, 2911–2917.
- (81) Serrano, G.; Reidy, S. M.; Zellers, E. T. Sens. Actuators, B 2009, 141. 217–226.
- (82) Radadia, A. D.; Masel, R. I.; Shannon, M. A.; Jerrell, J. P.; Cadwallader, K. R. *Anal. Chem.* **2008**, *80*, 4087–4094.
- (83) Nishino, M.; Takemori, Y.; Matsuoka, S.; Kanai, M.; Nishimoto, T.; Ueda, M.; Komori, K. *IEEJ Trans. Electr. Electron. Eng.* **2009**, *4*, 358–364.
- (84) Lewis, P. R.; Wheeler, D. R. Non-planar Microfabricated Gas Chromatography Column. U.S. Patent 7,273,517, September 25, 2007.
- (85) Bhushan, A.; Yemane, D.; Overton, E. B.; Goettert, J.; Murphy, M. C. J. Microelectromech. Syst. 2007, 16, 383–393.
- (86) Iwaya, T.; Akao, S.; Sakamoto, T.; Tsuji, T.; Nakaso, N.; Yamanaka, K. *Jpn. J. Appl. Phys.* **2012**, *51*, 07GC24.
- (87) Defiant Technologies. https://www3.epa.gov/ttnamti1/files/2014conference/posterlewis.pdf (accessed on September 20, 2018).
- (88) Raut, R. P.; Thurbide, K. B. Chromatographia **2017**, 80, 805–812.
- (89) Adkins, D. R.; Lewis, P. Folded Passage Gas Chromatography Column. U.S. Patent 8,635,901, January 28, 2014.
- (90) Noh, H. Parylene Microcolumn for Miniature Gas Chromatograph. Ph.D. Thesis, Georgia Institute of Technology, Atlanta, GA, 2004.
- (91) Lewis, A. C.; Hamilton, J. F.; Rhodes, C. N.; Halliday, J.; Bartle, K. D.; Homewood, P.; Grenfell, R. J.; Goody, B.; Harling, A. M.; Brewer, P. J. Chromatogr. A 2010, 1217, 768–774.
- (92) Navaei, M.; Mahdavifar, A.; Xu, J.; Dimandja, J.; McMurray, G.; Hesketh, P. ECS J. Solid State Sci. Technol. 2015, 4, S3011—S3015.
- (93) Radadia, A.; Salehi-Khojin, A.; Masel, R.; Shannon, M. J. Micromech. Microeng. 2010, 20, 015002.
- (94) Briscoe, C. G.; Yu, H.; Grodzinski, P.; Huang, R.-F.; Burdon, J. W. Multilayered Ceramic Micro-gas Chromatograph and Method for Making the Same. U.S. Patent 6,732,567, May 11, 2004.
- (95) Darko, E.; Thurbide, K. B.; Gerhardt, G. C.; Michienzi, J. Anal. Chem. 2013, 85, 5376-5381.
- (96) Zareian-Jahromi, M. A.; Ashraf-Khorassani, M.; Taylor, L. T.; Agah, M. J. Microelectromech. Syst. 2009, 18, 28–37.
- (97) Janik, A. J. Chromatogr. Sci. 1976, 14, 589-589.
- (98) Schisla, D.; Ding, H.; Carr, P.; Cussler, E. AIChE J. 1993, 39, 946–953.
- (99) De Malsche, W.; Eghbali, H.; Clicq, D.; Vangelooven, J.; Gardeniers, H.; Desmet, G. Anal. Chem. 2007, 79, 5915–5926.
- (100) De Malsche, W.; Op De Beeck, J.; De Bruyne, S.; Gardeniers, H.; Desmet, G. *Anal. Chem.* **2012**, *84*, 1214–1219.
- (101) Li, Y.; Du, X.; Wang, Y.; Tai, H.; Qiu, D.; Lin, Q.; Jiang, Y. RSC Adv. **2014**, *4*, 3742–3747.
- (102) Sun, J.; Cui, D.; Guan, F.; Chen, X.; Zhang, L. Sens. Actuators, B 2014, 201, 19-24.
- (103) Regmi, B. P.; Chan, R.; Agah, M. J. Chromatogr. A 2017, 1510, 66-72.
- (104) Sklorz, A.; Janßen, S.; Lang, W. Sens. Actuators, B 2013, 180, 43-49.
- (105) Sun, J.; Guan, F.; Zhu, X.; Ning, Z.; Ma, T.; Liu, J.; Deng, T. *J. Chromatogr. A* **2016**, *1429*, 311–316.
- (106) Cramers, C. A.; Janssen, H.-G.; van Deursen, M. M.; Leclercq, P. A. J. Chromatogr. A 1999, 856, 315–329.
- (107) Akbar, M.; Restaino, M.; Agah, M. Microsyst. Nanoeng. 2015, 1, 15039.
- (108) Reidy, S.; Lambertus, G.; Reece, J.; Sacks, R. Anal. Chem. 2006, 78, 2623–2630.

(109) Lin, Z.; Nuñovero, N.; Wang, J.; Nidetz, R.; Buggaveeti, S.; Kurabayashi, K.; Zellers, E. T. Sens. Actuators, B **2018**, 254, 561–572. (110) Sun, J.; Cui, D.; Li, Y.; Zhang, L.; Chen, J.; Li, H.; Chen, X. Sens. Actuators, B **2009**, 141, 431–435.

- (111) Whiting, J. J.; Fix, C. S.; Anderson, J. M.; Staton, A. W.; Manginell, R. P.; Wheeler, D. R.; Myers, E. B.; Roukes, M. L.; Simonson, R. In TRANSDUCERS 2009—International Conference on Solid-State Sensors, Actuators and Microsystems Conference; IEEE, 2009; pp 1666—1669.
- (112) Lee, C.-Y.; Liu, C.-C.; Chen, S.-C.; Chiang, C.-M.; Su, Y.-H.; Kuo, W.-C. Microsyst. Technol. 2011, 17, 523–531.
- (113) Cagliero, C.; Galli, S.; Galli, M.; Elmi, I.; Belluce, M.; Zampolli, S.; Sgorbini, B.; Rubiolo, P.; Bicchi, C. *J. Chromatogr. A* **2016**, *1429*, 329–339.
- (114) Boogaerts, T.; Verstappe, M.; Verzele, M. J. Chromatogr. Sci. 1972, 10, 217–219.
- (115) Regmi, B. P.; Chan, R.; Atta, A.; Agah, M. J. Chromatogr. A 2018, 1566, 124.
- (116) Kolesar, E.; Reston, R. J. Microelectromech. Syst. 1994, 3, 147–154.
- (117) Reid, V. R.; Stadermann, M.; Bakajin, O.; Synovec, R. E. *Talanta* **2009**, 77, 1420–1425.
- (118) Haudebourg, R.; Matouk, Z.; Zoghlami, E.; Azzouz, I.; Danaie, K.; Sassiat, P.; Thiebaut, D.; Vial, J. Anal. Bioanal. Chem. 2014, 406, 1245–1247.
- (119) Akbar, M.; Shakeel, H.; Agah, M. Lab Chip 2015, 15, 1748–1758.
- (120) Shakeel, H.; Agah, M. Sens. Actuators, B 2017, 242, 215-223.
- (121) Gross, G. M.; Nelson, D. A.; Grate, J. W.; Synovec, R. E. Anal. Chem. 2003, 75, 4558-4564.
- (122) Gross, G. M.; Grate, J. W.; Synovec, R. E. J. Chromatogr. A 2004, 1060, 225–236.
- (123) Zareian-Jahromi, M. A.; Agah, M. J. Microelectromech. Syst. 2010, 19, 294-304.
- (124) Read, D.; Sillerud, C. H. Metal-Organic Framework Thin Films as Stationary Phases in Microfabricated Gas-Chromatography Columns; Sandia Report SAND2016-0706; Sandia National Laboratories (SNL-NM): Albuquerque, NM, 2016.
- (125) Gu, Z.-Y.; Yang, C.-X.; Chang, N.; Yan, X.-P. Acc. Chem. Res. 2012, 45, 734-745.
- (126) Gu, Z. Y.; Yan, X. P. Angew. Chem., Int. Ed. 2010, 49, 1477-1480
- (127) Xie, S.-M.; Zhang, Z.-J.; Wang, Z.-Y.; Yuan, L.-M. J. Am. Chem. Soc. 2011, 133, 11892–11895.
- (128) Ragonese, C.; Sciarrone, D.; Tranchida, P. Q.; Dugo, P.; Mondello, L. J. Chromatogr. A **2012**, 1255, 130–144.
- (129) Hantao, L. W.; Najafi, A.; Zhang, C.; Augusto, F.; Anderson, J. L. Anal. Chem. 2014, 86, 3717–3721.
- (130) Han, X.; Armstrong, D. W. Acc. Chem. Res. 2007, 40, 1079-1086.
- (131) Ding, J.; Welton, T.; Armstrong, D. W. Anal. Chem. 2004, 76, 6819–6822.
- (132) Dettmer, K. Anal. Bioanal. Chem. 2014, 406, 4931-4939.
- (133) Ragonese, C.; Sciarrone, D.; Tranchida, P. Q.; Dugo, P.; Dugo, G.; Mondello, L. *Anal. Chem.* **2011**, *83*, 7947–7954.
- (134) Poole, C. F.; Poole, S. K. J. Sep. Sci. 2011, 34, 888-900.
- (135) Trujillo-Rodríguez, M. J.; Pacheco-Fernández, I.; Rincón, A. A.; Afonso, A. M.; Pino, V. In *Analytical Applications of Ionic Liquids*; World Scientific, 2017; pp 45–82.
- (136) Qin, Y.; Gianchandani, Y. B. J. Micromech. Microeng. 2014, 24, 065011.
- (137) Staples, E. J.; Viswanathan, S. IEEE Sens. J. 2005, 5, 622-631.
- (138) Yost, R. A.; Hail, M. E. Direct Resistive Heating and Temperature Measurement of Metal-clad Capillary Columns in Gas Chromatography and Related Separation Techniques. U.S. Patent 5,114,439, May 19, 1992.
- (139) AZO Materials. https://www.azom.com/article.aspx?ArticleID=13818 (accessed on September 21, 2018).
- (140) Ehrmann, E.; Dharmasena, H.; Carney, K.; Overton, E. J. Chromatogr. Sci. 1996, 34, 533–539.

- (141) Kim, S. K.; Chang, H.; Zellers, E. T. *Anal. Chem.* **2011**, 83, 7198–7206.
- (142) Kim, S.-J.; Reidy, S. M.; Block, B. P.; Wise, K. D.; Zellers, E. T.; Kurabayashi, K. *Lab Chip* **2010**, *10*, 1647–1654.
- (143) Robinson, A. L.; Anderson, L. F. Sub-to Super-ambient Temperature Programmable Microfabricated Gas Chromatography Column. U.S. Patent 6,706,091, March 16, 2004.
- (144) Manginell, R. P.; Frye-Mason, G. C.; Kottenstette, R.; Lewis, P. R.; WONG, C. C. Microfabricated planar preconcentrator; Sandia National Laboratories: Albuquerque, NM, 2000.
- (145) Manginell, R. P.; Adkins, D. R.; Sokolowski, S. S.; Lewis, P. R. Non-planar Chemical Preconcentrator. U.S. Patent 7,118,712, October 10, 2006.
- (146) Tian, W.-C.; Pang, S. W.; Lu, C.-J.; Zellers, E. T. J. Microelectromech. Syst. 2003, 12, 264–272.
- (147) Tian, W.-C.; Chan, H. K.; Lu, C.-J.; Pang, S. W.; Zellers, E. T. J. Microelectromech. Syst. **2005**, 14, 498–507.
- (148) Kim, S.; Chang, H.; Zellers, E. In TRANSDUCERS 2009—International Conference on Solid-State Sensors, Actuators and Microsystems; IEEE, 2009; pp 128–131.
- (149) Zhong, Q.; Steinecker, W. H.; Zellers, E. T. Analyst 2009, 134, 283–293.
- (150) Alfeeli, B.; Cho, D.; Ashraf-Khorassani, M.; Taylor, L. T.; Agah, M. Sens. Actuators, B 2008, 133, 24–32.
- (151) Akbar, M.; Wang, D.; Goodman, R.; Hoover, A.; Rice, G.; Heflin, J. R.; Agah, M. *J. Chromatogr. A* **2013**, *1322*, 1–7.
- (152) Dow, A. B. A.; Lang, W. Sens. Actuators, B 2010, 151, 304-307.
- (153) Seo, J. H.; Kim, S. K.; Zellers, E. T.; Kurabayashi, K. Lab Chip **2012**, 12, 717–724.
- (154) Cruz, D.; Chang, J.; Showalter, S.; Gelbard, F.; Manginell, R.; Blain, M. Sens. Actuators, B 2007, 121, 414-422.
- (155) Williams, D.; Pappas, G. Field Anal. Chem. Technol. **1999**, 3, 45–53.
- (156) Whiting, J. J.; Lu, C.-J.; Zellers, E. T.; Sacks, R. D. Anal. Chem. **2001**, 73, 4668–4675.
- (157) Electronic Sensor Technology, http://www.estcal.com/blog/real-time-chemical-process-measurements-using-gcsaw-system (accessed on September 21, 2018).
- (158) Cai, Q.-Y.; Zellers, E. T. Anal. Chem. 2002, 74, 3533-3539.
- (159) Patel, S.; Mlsna, T.; Fruhberger, B.; Klaassen, E.; Cemalovic, S.; Baselt, D. Sens. Actuators, B 2003, 96, 541-553.
- (160) Li, M.; Myers, E.; Tang, H.; Aldridge, S.; McCaig, H.; Whiting, J.; Simonson, R.; Lewis, N.; Roukes, M. *Nano Lett.* **2010**, *10*, 3899–3903.
- (161) Sun, J.; Guan, F.; Cui, D.; Chen, X.; Zhang, L.; Chen, J. Sens. Actuators, B 2013, 188, 513-518.
- (162) Zhu, H.; Nidetz, R.; Zhou, M.; Lee, J.; Buggaveeti, S.; Kurabayashi, K.; Fan, X. Lab Chip 2015, 15, 3021–3029.
- (163) Narayanan, S.; Rice, G.; Agah, M. Sens. Actuators, B 2015, 206, 190–197.
- (164) Zhu, H.; Zhou, M.; Lee, J.; Nidetz, R.; Kurabayashi, K.; Fan, X. *Anal. Chem.* **2016**, *88*, 8780–8786.
- (165) Zimmermann, S.; Wischhusen, S.; Müller, J. Sens. Actuators, B **2000**, 63, 159–166.
- (166) Hayward, T. C.; Thurbide, K. B. *J. Chromatogr. A* **2008**, *1200*, 2–7
- (167) Kuipers, W.; Müller, J. J. Chromatogr. A 2011, 1218, 1891–
- (168) Kim, J.; Bae, B.; Hammonds, J.; Kang, T.; Shannon, M. A. Sens. Actuators, B **2012**, 168, 111–117.
- (169) Poole, C. J. High Resolut. Chromatogr. 1982, 5, 454-471.
- (170) Klee, M. S.; Williams, M. D.; Chang, I.; Murphy, J. J. High Resolut. Chromatogr. 1999, 22, 24–28.
- (171) von Mühlen, C.; Khummueng, W.; Alcaraz Zini, C.; Bastos Caramão, E.; Marriott, P. I. *J. Sep. Sci.* **2006**, *29*, 1909–1921.
- (172) Miller, R. A.; Nazarov, E. G.; Eiceman, G. A.; King, A. T. Sens. Actuators, A 2001, 91, 301–312.
- (173) Eiceman, G.; Nazarov, E.; Miller, R.; Krylov, E.; Zapata, A. Analyst **2002**, 127, 466–471.

- (174) Lambertus, G. R.; Fix, C. S.; Reidy, S. M.; Miller, R. A.; Wheeler, D.; Nazarov, E.; Sacks, R. *Anal. Chem.* **2005**, *77*, 7563–7571.
- (175) Lewis, P. R.; Manginell, P.; Adkins, D. R.; Kottenstette, R. J.; Wheeler, D. R.; Sokolowski, S. S.; Trudell, D. E.; Byrnes, J. E.; Okandan, M.; Bauer, J. M. *IEEE Sens. J.* **2006**, *6*, 784–795.
- (176) Frye-Mason, G.; Kottenstette, R.; Mowry, C.; Morgan, C.; Manginell, R.; Lewis, P.; Matzke, C.; Dulleck, G.; Anderson, L.; Adkins, D. In *Micro Total Analysis Systems* 2001; Springer, 2001; pp 658–660. (177) Sandia National Laboratories Annual Report 2002/2003.
- (178) Zhong, Q.; Veeneman, R. A.; Steinecker, W. H.; Jia, C.; Batterman, S. A.; Zellers, E. T. J. Environ. Monit. 2007, 9, 440–448.
- (179) Collin, W. R.; Serrano, G.; Wright, L. K.; Chang, H.; Nuñovero, N. s.; Zellers, E. T. *Anal. Chem.* **2014**, *86*, 655–663.
- (180) Zellers, E. T.; Reidy, S.; Veeneman, R. A.; Gordenker, R.; Steinecker, W. H.; Lambertus, G. R.; Kim, H.; Potkay, J. A.; Rowe, M. P.; Zhong, Q. In TRANSDUCERS 2007–2007 International Solid-State Sensors, Actuators and Microsystems Conference; IEEE, 2007; pp 1491–1496.
- (181) Agah, M.; Lambertus, G. R.; Sacks, R.; Wise, K. J. Microelectromech. Syst. 2006, 15, 1371-1378.
- (182) Nair, S. N. S. MicroGC: Of Detectors and Their Integration. Ph.D. Dissertation, Virginia Tech, Blacksburg, VA, 2014.
- (183) Collin, W. R.; Scholten, K. W.; Fan, X.; Paul, D.; Kurabayashi, K.; Zellers, E. T. *Analyst* **2016**, *141*, 261–269.
- (184) Liu, J.; Seo, J. H.; Li, Y.; Chen, D.; Kurabayashi, K.; Fan, X. *Lab Chip* **2013**, *13*, 818–825.
- (185) Kim, S.-J.; Serrano, G.; Wise, K. D.; Kurabayashi, K.; Zellers, E. T. Anal. Chem. **2011**, 83, 5556–5562.
- (186) Serrano, G.; Paul, D.; Kim, S.-J.; Kurabayashi, K.; Zellers, E. T. Anal. Chem. 2012, 84, 6973–6980.
- (187) Collin, W. R.; Nuñovero, N.; Paul, D.; Kurabayashi, K.; Zellers, E. T. *J. Chromatogr. A* **2016**, *1444*, 114–122.
- (188) Blumberg, L. M. J. Sep. Sci. 2008, 31, 3358-3365.
- (189) Fan, X. In Sensors; IEEE, 2013; pp 1-3.
- (190) Grob, K.; Grob, G.; Grob, K., Jr J. Chromatogr. A 1981, 219, 13–20.
- (191) Luong, J.; Gras, R.; Jennings, W. J. Sep. Sci. 2007, 30, 2480–2492